INSTITUTE OF PLASMA PHYSICS

NAGOYA UNIVERSITY

RESEARCH REPORT

NAGOYA, JAPAN

THEORY AND EXPERIMENT ON RF PLUGGING OF MAGNETICALLY CONFINED PLASMA IN AN OPEN-ENDED SYSTEM

Tetsuo Watari, Shinji Hiroe,
Teruyuki Sato and Setsuo Ichimaru*

IPPJ-191 April 1974

Further communication about this report is to be sent to the Research Information Center, Institute of Plasma Physics, Nagoya University, Nagoya, Japan.

Permanent address:
* Department of Physics, University of Tokyo, Tokyo, Japan.

ABSTRACT

The theory of an r.f. plugging of a magnetically confined plasma in an open-ended system is presented; it takes explicit account of the collective effect brought about by the dynamic screening action of the plasma. The theory predicts a maximum efficiency of the r.f. plugging at an optimum frequency corresponding to a zero of the longitudinal dielectric constant. The plugging efficiency is calculated as a function of the plasma density, the strength of the r.f. field, and the intensity of the magnetic field. These theoretical predictions are compared with the experimental observations, demonstrating a satisfactory agreement in overall features. The results provide a useful scaling law associated with the concept of the r.f. confinement. The theory also offers an adequate explanation for the discrepancy between the experimental values of the optimum frequency and those predicted by a conventional theory based on an individual-particle model.

I. INTRODUCTION

When an r.f. electric field is applied in a direction perpendicular to a magnetic field, the combined effect of the electric field and a spatial variation of the magnetic field is such as to exert a force field on a charged particle in the direction of decreasing magnetic field. According to the calculation originally carried out by Dow and Krechetli,[1] this force may be expressed as

$$\underset{\sim}{F} = -\underset{\sim}{\nabla}\,\phi \qquad (1)$$

with a potential function defined by

$$\phi = \frac{q^2 E^2}{4m}\,\frac{1}{\omega^2 - \omega_c^2}$$

Here, q and m denote the electric charge and mass of the particle involved; $\omega_c = qB/mc$ is the cyclotron frequency; ω and E are the frequency and the intensity of the externally applied r.f. field. Consoli and his collaborators[2] attempted to use this concept for an acceleration of the electrons.

The physical origin of the force (1) may be understood in the following way: Consider a situation as described in Fig.1; a charged particle is placed in a slowly converging magnetic field and a uniform r.f. electric field is applied to it. Associated with such a field configuration, a component $B_\perp$ of the magnetic field perpendicular to the magnetic axis arises; this field component coupled with a

perpendicular velocity component $\underset{\sim}{v_\perp}$ of the particle produces a Lorentz force toward weaker magnetic field, an effect well known as the mechanism of the magnetic-mirror reflection. In the presence of the r.f. field, the perpendicular velocity and the Larmor radius $r_\perp$ of the particle will increase and may diverge at a resonant condition. Since $B_\perp$ acting on the particle is proportional to $r_\perp$, the resulting force should be enhanced accordingly; a calculation shows

$$\underset{\sim}{F} = -\frac{q^2 E^2}{2m} \frac{\omega_c^2}{(\omega^2 - \omega_c^2)^2} \frac{\nabla_\parallel B_\parallel}{B_\parallel} \qquad (2)$$

Equation (1) reduces to this expression when a uniform r.f. field is assumed.

A series of experimental investigations have been carried out in the past several years to clarify such a plugging effect of the r.f. field on a plasma confined in a cusped magnetic field.[3-9] In the course of these experiments, however, there appeared phenomena which could not be explained simply in terms of Eq.(1). The physical origin of such a discord may be traced to the collective response of the plasma; in the experiment we are actually treating a collection of charged particles in a plasma state, while Eq.(1) is based on a consideration of the behavior of a single particle in the r.f. field.

The purpose of the present paper is, therefore, to develop a plasma theory of the r.f. plugging with inclusion of the collective effects inherent in the plasma. A number of predictions are thus made on the detailed properties of

the r.f. plugging of the ions within a collective model. These predictions are then compared with experimental results, demonstrating thereby outstanding features of the collective model.

II. FORMULATION OF THE THEORY

Consider a plasma in a slowly converging magentic field; an r.f. field is applied to it through a pair of parallel-plate electrodes. The dielectric shielding effect of the plasma then acts to modify the electric field inside it. Such an effect may be described with the aid of the frequency and wave-vector dependent (longitudinal) dielectric constant $\varepsilon(\underset{\sim}{k}, \omega)$ as

$$\underset{\sim}{E}(\underset{\sim}{r}, t) = \int_{-\infty}^{+\infty} d\omega \int_{-\infty}^{+\infty} d\underset{\sim}{k}\ \underset{\sim}{E}(\underset{\sim}{k}, \omega)\ \exp\left[i(\underset{\sim}{k}\cdot\underset{\sim}{r} - \omega t)\right], \tag{3}$$

$$\underset{\sim}{E}(\underset{\sim}{k}, \omega) = \frac{\underset{\sim}{E}_{ext}(\underset{\sim}{k}, \omega)}{\varepsilon(\underset{\sim}{k}, \omega)}, \tag{4}$$

where $\underset{\sim}{E}_{ext}(\underset{\sim}{k}, \omega)$ is the Fourier component of the vacuum r.f. field $\underset{\sim}{E}_{ext}(\underset{\sim}{r}, t)$ produced by the electrodes. In adopting the expression (4), we are assuming that the major effect of the plasma can be represented by its longitudinal response; the effects of transverse response are not considered in this paper.

We begin with the equation of motion for a charged particle in the system; we separate the perpendicular and parallel components of the equation with respect to the major direction of the magnetic field:

$$\frac{d\underset{\sim}{v}_{\perp}}{dt} = \frac{q}{m}\underset{\sim}{E}(\underset{\sim}{r},t) - \frac{q}{mc}[\underset{\sim}{v}\times\underset{\sim}{B}_{\parallel}] \quad , \qquad (5)$$

$$\underset{\sim}{F} = m\frac{d\underset{\sim}{v}_{\parallel}}{dt} = \frac{q}{c}\left[\underset{\sim}{v}_{\perp}(t)\times\underset{\sim}{B}_{\perp}[\underset{\sim}{r}_{\perp}(t),t]\right] - q\underset{\sim}{E}(\underset{\sim}{r},t) \quad , \qquad (6)$$

Equation (5) describes the cyclotron motion of the particle in the presence of the forced oscillatory electric field. The retarding force acting on the particle may then be determined from Eq.(6). The last term in Eq.(6) represents the effect of the parallel electric field produced by a possible nonuniformity in the r.f. field along the magnetic field. Such a nonuniformity is known to produce little effect[10] on the r.f. plugging under the present investigation; we shall henceforce ignore the last term of Eq.(6).

Integrations of Eq.(5) with respect to time formally yield[11]

$$\underset{\sim}{v}(t) = \underset{\approx}{B}(t-t_o)\cdot\underset{\sim}{v}(t_o) + \frac{q}{m}\int_{t_o}^{t} dt'\,\underset{\approx}{B}(t-t')\cdot\underset{\sim}{E}[\underset{\sim}{r}(t'),t'] \quad , \qquad (7)$$

$$\underset{\sim}{r}(t) = \underset{\sim}{r}(t) - \frac{1}{\omega_c}\underset{\approx}{H}(t-t_o)\cdot\underset{\sim}{v}(t_o) - \frac{c}{B}\int_{t_o}^{t} dt'\,\underset{\approx}{H}(t-t')\,\underset{\sim}{E}[\underset{\sim}{r}(t'),t'] \quad , \qquad (8)$$

where $\underset{\sim}{r}(t_o)$ and $\underset{\sim}{v}(t_o)$ denote the position and the velocity of the particle at an initial time t_o; tensors involved in Eqs.(7) and (8) are defined so that

$$\underset{\approx\approx}{H}(t) = \begin{bmatrix} \sin\omega_c t & 1-\cos\omega_c t & 0 \\ -(1-\cos\omega_c t) & \sin\omega_c t & 0 \\ 0 & 0 & \omega_c t \end{bmatrix}, \tag{9}$$

$$\underset{\approx\approx}{B}(t) = \begin{bmatrix} \cos\omega_c t & \sin\omega_c t & 0 \\ -\sin\omega_c t & \cos\omega_c t & 0 \\ 0 & 0 & 1 \end{bmatrix}, \tag{10}$$

The effects of the r.f. field on the cyclotron motion of the particle are contained in the last terms on the right-hand sides of Eqs.(7) and (8). These terms, in turn, depend on the exact particle orbit r(t) in the presence of the electric field.

The complex situation arising from such an interdependence of physical variables may be simplified in our calculation; we are interested in obtaining the expression of the parallel force to the first order in $|E|^2$ as in the case of Eq.(1). Hence, we may carry out perturbation-theoretical expansion of Eqs.(7) and (8) with respect to the electric-field strength; we retain the terms up to the first order in the expansion. The particle orbit entering the last terms of Eqs.(7) and (8) may thus be replaced by the unperturbed cyclotron orbit,

$$\underset{\sim}{R}_0(t) = \underset{\sim}{r}(t_0) + (1/\omega_c)\,\underset{\approx}{H}(t-t_0)\cdot\underset{\sim}{v}(t_0)\,, \qquad (11)$$

Substituting Eqs.(7) and (8) into Eq.(6) and carrying out a time average, we obtain

$$\overline{\underset{\sim}{F}_{\parallel}} = \frac{q}{c}\overline{\left[\underset{\sim}{v}_{\perp th}\times\left(\Delta\underset{\sim}{r}_{th}\cdot\underset{\sim}{\nabla}\,\underset{\sim}{B}_{\perp}\right)\right]} + \frac{q}{c}\overline{\left[\underset{\sim}{v}_{\perp E}\times\left(\Delta\underset{\sim}{r}_{E}\cdot\underset{\sim}{\nabla}\,\underset{\sim}{B}_{\parallel}\right)\right]}\,, \qquad (12)$$

where

$$\underset{\sim}{v}_{\perp th} = \underset{\approx}{B}(t-t_0)\cdot\underset{\sim}{v}(t_0) \qquad (13)$$

$$\Delta\underset{\sim}{r}_{th} = (1/\omega_c)\,\underset{\approx}{H}(t-t_0)\cdot\underset{\sim}{v}(t_0)\,, \qquad (14)$$

$$\underset{\sim}{v}_{\perp E} = \frac{q}{m}\int_{t_0}^{t} dt'\;\underset{\approx}{B}(t-t')\cdot\underset{\sim}{E}\left[\underset{\sim}{R}_0(t'),\,t'\right]\,, \qquad (15)$$

$$\Delta\underset{\sim}{r}_{th} = \frac{q}{m}\int_{t_0}^{t} dt'\;\underset{\approx}{H}(t-t')\cdot\underset{\sim}{E}\left[\underset{\sim}{R}_0(t'),\,t'\right]\,. \qquad (16)$$

The separation into two physically distinct terms on the right-hand side of Eq.(12) stems from the assumption that there is a frequency mismatch, greater than the inverse of the period of the field-particle interaction, between the frequency ω of the applied electric field and the cyclotron frequency ω_c.

III. DETAILED CALCULATION

In order to calculate Eq.(12) explicitly we now adopt the configuration as shown in Fig.2. All the quantities are uniform in the direction of the y-axis. The major direction of the magnetic field is along the z-axis; the magnetic lines of force may have small curvature on the x-z plane.

A particle injected at z = 0 travels along a magnetic line of force and experiences a retarding force under the parallel electrodes. For the configuration of Fig.2, Eq.(12) can be written as

$$F = -\frac{q}{c}\overline{v_y \Delta x}\,\frac{\partial B_x}{\partial x} = \frac{q}{c}\overline{v_y \Delta x}\,\frac{\partial B_z}{\partial z} \qquad (17)$$

where the relation div B = 0 is used. It is easy to calculate $v_{y,th}$ and Δx_{th} from Eqs.(13) and (14); substitution of these expressions into (17) yields the force

$$F_{th} = -\frac{m}{2}\frac{(v_\perp)^2}{B}\frac{\partial B_\perp}{\partial z}$$

where $v_\perp^o = ((v_x^o)^2 + (v_y^o)^2)^{1/2}$ is the initial speed of a particle perpendicular to the z-axis. We employ the superscript 0 to designate an initial value of the corresponding variable.

The retarding force arising from the r.f. field is obtained in the same way by substituting $v_{y,E}$ and Δx_E in Eq.(12). The unperturbed orbit $\underset{\sim}{R}_o(t)$ in the integrands of Eqs.(15) and (16) may be expressed as follows:

$$\underset{\sim}{R}_0(t) = R_{0x}\hat{x} + R_{0y}\hat{y} + R_{0z}\hat{z} , \qquad (18)$$

with

$$R_{0x}(t) = (x^\circ + v_y^\circ/\omega_c) + (v_\perp^\circ/\omega_c)\sin(\omega_c t - \varphi^\circ) , \qquad (19)$$

$$R_{0y}(t) = (y^\circ - v_x^\circ/\omega_c) + (v_\perp^\circ/\omega_c)\cos(\omega_c t - \varphi^\circ) , \qquad (20)$$

$$\varphi^\circ = \tan^{-1}(v_y^\circ/v_x^\circ) ,$$

$$R_{0z}(t) = z^\circ + v_z^\circ t . \qquad (21)$$

Here, $\hat{x}$, $\hat{y}$, and $\hat{z}$ denote the unit vectors in the directions of x-, y-, and z-axes, respectively.

We now single out a Fourier component of the electric field $E(\underset{\sim}{r}, t)$ with a wave vector $\underset{\sim}{k} = k_x\hat{x} + k_z\hat{z}$ and a frequency ω in Eq.(3). Along the unperturbed orbit (18), we then have

$$E_x[\underset{\sim}{R}_0(t), t] = \frac{E_{ext}(k_x, k_z, \omega)}{\varepsilon(k_x, k_z, \omega)} \times \exp\{i[k_z z^\circ + k_x(x^\circ + v_y^\circ/\omega_c)]\} \times \sum_{\nu=-\infty}^{\nu=\infty} J_\nu\left(\frac{k_x v_\perp^\circ}{\omega_c}\right) \exp[i(k_z v_z^\circ - \omega)t + i\nu(\omega_c t - \varphi^\circ)] \qquad (22)$$

Substituting (22) into (15) and (16), and executing the integration, we find that $v_{y,E}$ and Δx_E are obtained as

$$v_{y,E} = \frac{q}{2m} \frac{E_{ext}(k_x, k_z, \omega)}{\varepsilon(k_x, k_z, \omega + i\eta)} \sum_{\nu=-\infty}^{\nu=\infty} J_\nu\left(\frac{k_x v_\perp^\circ}{\omega_c}\right)$$

$$\times \exp\left[ik_x(x^\circ + v_y^\circ/\omega_c) + ik_z z^\circ + i(k_z v_z^\circ - \omega + \nu\omega_c)t - i\nu\varphi^\circ\right]$$

$$\times \left\{ \frac{1}{k_z v_z^\circ - (\omega + i\eta) + (\nu-1)\omega_c} - \frac{1}{k_z v_z^\circ - (\omega + i\eta) + (\nu+1)\omega_c} \right\} \quad (23)$$

$$\Delta x_E = -v_{y,E} / \omega_c \quad , \quad (24)$$

where η is a positive infinitesimal which ensures a causal response of the system. Equations (23) and (24) represent the linear response of v_y and Δx to a monochromatic disturbance with space-time variation $\exp\{i(k_x x + k_z z - \omega t)\}$; relevant linear combination of these monochromatic variation should then provide an actual behavior.

Substitution of Eqs.(23) and (24) into Eq.(17) gives us the expression of the force as a function of the initial conditions of the particle, i.e., z°, $x^\circ + v_y^\circ/\omega_c$, v_z°, $v_\perp^\circ$, and ϕ°. We thus carry out an average over these initial conditions. Let us denote such an average by a symbol $\langle\ \rangle$. Carrying out the average of $v_y \Delta x$ over z°, $x^\circ + v_y^\circ/\omega_c$, and ϕ° as well as the time average, we obtain

$$\langle v_y \Delta x \rangle = \int dk_x \int dk_z \int d\omega \left(-\frac{cq}{Bm}\right) \frac{|E_{ext}(k_x, k_z, \omega)|^2}{|\varepsilon(k_x, k_z, \omega)|^2}$$

$$\times \sum_{\nu=-\infty}^{\nu=\infty} J_\nu^2\left(\frac{k_x v_\perp^\circ}{\omega_c}\right) \left\{ \frac{2\omega_c}{(k_z v_z^\circ - \omega + \nu\omega_c)^2 - \omega_c^2} \right\}^2 \quad , \quad (25)$$

Equation (25) still contains the initial condition for $v_\perp$ in the arguments of the Bessel functions; it implies that a particle with a large $v_\perp$ is sensitive to higher-harmonic effect. The initial condition v_z^o is also involved in the denominator of Eq.(25), describing the Doppler effect arising from the parallel motion. Let us thus denote the further average including these variables by a symbol << >>. Assuming a Maxwellian distribution of the particles, we carry out the average of Eq.(25) over $v_\perp^o$ and v_z^o. We then substitute the result into Eq.(17), obtaining thereby the final expression for the averaged value of the force as

$$\overline{\langle\langle F \rangle\rangle} = \frac{q}{c} \overline{\langle\langle v_y \Delta x \rangle\rangle} \frac{\partial B_z}{\partial z}$$

$$= (2\pi)^3 \frac{q^2}{m} \int dk_x \int dk_z \int d\omega \sum_{\nu=-\infty}^{\nu=\infty} \frac{|E_{ext}(k_x, k_z, \omega)|^2}{|\varepsilon(k_x, k_z, \omega)|^2}$$

$$\times \frac{\pi^{1/2}}{(k_z v_\perp)^2} e^{-Z} \mathcal{J}_m \left\{ (I_{\nu+1} + I_{\nu-1}) W_\nu' - \left(\frac{k_z v_T}{\omega_c}\right)(I_{\nu+1} - I_{\nu-1}) W_\nu \right\} \frac{1}{B_z} \frac{\partial B_z}{\partial z} \qquad (26)$$

Here

$$W(\zeta) = \frac{-i}{\pi} \int_{-\infty}^{\infty} \frac{e^{-x^2}}{x - \zeta} dx \quad , \quad \zeta_\nu = (\omega - \nu\omega_c)/k_z v_T \quad ,$$

$$v_T^2 = 2T/m \quad , \quad Z = \frac{1}{2} k_x^2 \rho^2 \quad , \quad \rho^2 = v_T^2/\omega_c^2 \quad ,$$

and, we have suppressed the arguments of the functions $I_\nu(Z)$ and $W(\zeta_\nu)$.

IV. RETARDING FORCE IN THE EXPERIMENTAL CONDITION

Equation (26) gives the expression for the force in the presence of an electric field. To compare the theory with our experimental results, we must take account of the experimental conditions into the theoretical results. In the experiment, an r.f. voltage is applied through a pair of parallel-plate electrodes with width ΔL and separation d (see Fig.2). The quantity $E_{ext}(k_x, k_z, \omega)$ should thus be regarded as a Fourier component of the vacuum field created in this way. Consequently $E_{ext}(k_x, k_z, \omega)$ takes on a sizable magnitude when k_x and k_z satisfy the following conditions:

$$k_x = (2\ell_1 + 1)\pi / d \quad , \tag{27}$$

$$k_z = (2\ell_2 + 1)\pi / \Delta L \quad , \tag{28}$$

where ℓ_1 and ℓ_2 are arbitrary integers. On the other hand, in a bounded plasma as shown in Fig.3, the boundary condition specifies the wave number k_x to be

$$k_x = (2\ell_3 + 1)\pi / h \quad , \tag{29}$$

where h denotes the thickness of the plasma and ℓ_3 is an arbitrary integer. We may then assume that the fundamental mode carries the bulk of the field strength in a plasma; we thus select the value of k_x, and hence that of ℓ_1, satisfying

$$k_x = \pi/h = (2\ell_1 + 1)\,\pi/d \qquad (30)$$

The component k_z can take on various values in accord with Eq.(28); since the field dissipation increases with k_z, however, we are again led to select the mode with $\ell_2 = 0$:

$$k_z = \pi/\Delta L \,. \qquad (31)$$

A more accurate treatment pertaining to the eigenmodes of bounded plasmas has been made by Watanabe and Hatori.[12] Here, however, we are contented with these simple approximations, which describe the experimental situation to a good degree of accuracy.

With inclusion of the constraints (30) and (31), we may express

$$|E_{ext}(k_x, k_z, \omega)|^2 = 2^{-9}\pi^{-3}E_0^2\{\delta(\omega-\omega_{rf}) + \delta(\omega+\omega_{rf})\}$$

$$\times\{\delta(k_x-k_\perp)+\delta(k_x+k_\perp)\}\{\delta(k_z-k_\parallel)+\delta(k_z+k_\parallel)\}\,. \qquad (32)$$

where

$$E_0 = V_{rf}/d\,,\quad k_\parallel = \pi/\Delta L\,,\quad \text{and}\quad k_\perp = \pi/h\,,$$

In our experiments, $\Delta L >> h$ so that we assume $k_\perp >> k_\parallel$. Substituting Eq.(32) into Eq.(26) and executing integration, we obtain the force expressed in a form comparable

with our experiment:

$$\overline{\langle\langle F \rangle\rangle} = \frac{q^2}{m}\left(\frac{1}{2}\right)^3 \sum_{\nu=-\infty}^{\nu=\infty} \frac{E_0^2}{|\varepsilon(k_\perp, k_\parallel, \omega)|^2} \frac{\pi^{1/2}}{(k_\parallel v_T)^2} e^{-Z}$$

$$\times \mathrm{Im}\left\{ (I_{\nu+1} + I_{\nu-1}) W_\nu' - (k_\parallel v_T/\omega)(I_{\nu+1} - I_{\nu-1}) W_\nu \right\} \frac{\partial B_z}{\partial z} \qquad (33)$$

Here,

$$I_\nu = I_\nu(Z) \quad , \quad Z = k_\perp^2 T/m\omega_c^2 \quad ,$$

$$W_\nu = W(\zeta_\nu) \quad , \quad \zeta_\nu = (\omega - \nu\omega_c)/k_\parallel v_T \quad ,$$

and the r.f. frequency ω_{rf} applied through the electrodes is simply denoted by ω. In addition to Eq.(33), we need an explicit expression for the longitudinal dielectric constant, that is,

$$\varepsilon(k_\perp, k_\parallel, \omega) = 1 - \sum \frac{k_D^2}{k^2}\left(1 + i\pi^{1/2}\frac{\omega}{k_\parallel v_T}\sum_{\nu=-\infty}^{\nu=\infty} I_\nu e^{-Z} W_\nu\right) \qquad (34)$$

where

$$k_D^2 = 4\pi n e^2/T$$

Equation (34), depending on the density of the plasma, describes the characteristic effects of the collective phenomena in the plasma. The degree of approximation involved in the derivation of Eq.(34) is the same as that involved in Eq.(33).

In our experimental condition we may assume $\zeta_{\nu i} >> 1$ for the ions except in the very vicinity of $\omega = \nu\omega_{ci}$. We may thus carry out an asymptotic expansion of the dispersion function involved in Eq.(33). Then the expression is simplified as follows:

$$\ll F \gg \; = \; F_1 \cdot F_2 \cdot F_3 \; , \tag{35}$$

where

$$F_1 = - \frac{q^2 E_0^2}{4 m \omega_c^2} \frac{\nabla B}{B} \tag{36}$$

$$F_2 = \sum_{\nu} \frac{\omega_c^4}{\{ (\omega - \nu \omega_c)^2 - \omega_c^2 \}^2} I_\nu e^{-Z} \tag{37}$$

$$F_3 = \frac{1}{| \varepsilon(k_\perp , k_\parallel , \omega) |^2} \tag{38}$$

The same approximation must be adopted in the expression of $\varepsilon(k_\perp, k_\parallel, \omega)$ in Eq.(34); hence we have

$$\varepsilon(K_\perp, K_\parallel, \omega) = 1 - 2 \frac{k_{Di}^2}{K^2} \sum_{\nu=-\infty}^{\nu=\infty} \frac{\nu^2 \omega_{ci}^2}{\omega^2 - \nu^2 \omega_{ci}^2} I_\nu e^{-Z_i}$$
$$+ i \sqrt{\pi} \frac{k_{Di}^2}{K^2} \frac{\omega}{k_\parallel v_{Ti}} \sum_{\nu=-\infty}^{\nu=+\infty} I_\nu e^{-Z_i} \exp(-\zeta_{\nu i}^2) \tag{39}$$

In Eq.(39), we have neglected the shielding effect of the electrons; the electrons may be viewed as being confined in a thin layer with a thickness comparable to their Larmor radii, and thereby regarded as producing no significant effect in the main volume of our experiment.

It is clear that Eq.(2) may be derived as a special case of Eq.(35). The factor F_3 reduces to 1 in the low density limit; no dielectric screening effects exist there and the vacuum field remains. When $k_\perp$ or T approaches zero, we have $I_\nu(z) = \delta_{\nu,o}$, Kronecker's delta; Eq.(37) is then written as $F_2 = \omega_c^4/(\omega^2 - \omega_c^2)^2$. Substitution of these expressions into Eq.(35) yields Eq.(2). Thus we observe that Eq.(35) is a correct generalization of Eq.(2); both the collective effect of the plasma and the finite Larmor-radius effect are now taken into consideration.

V. OPTIMUM FREQUENCY

Equations (35)-(38) describe the frequency dependence of the retarding force. The term F_1 has the dimension of the force, while F_2 and F_3 are dimensionless quantities. The functions F_2 and F_3 exhibit certain resonant structures as functions of the r.f. frequency; we may thus define an optimum frequency as that corresponding to a maximum value of the force. In these connections, it is interesting to know which of the two factors would actually be responsible for the optimum frequency. It is clear from the derivation of Eq.(35) that F_2 is related to the force produced by the vacuum r.f. field, while F_3 describes the dielectric screening effects of the plasma. To elucidate this point in detail, we carry out numerical computations of the functions F_2, F_3, and the product $F_2 \cdot F_3$; the results are shown in Figs.4-6. The computational result of F_2 shown in Fig.4 suggests that the force would be enhanced at the

cyclotron frequency and its harmonics. Appearance of these harmonics represents finite Larmor-radius effects taken into account in the present theory. Figure 5 shows the numerical computation of ε_1, the real part of the dielectric constant. As long as the imaginary part of the dielectric constant ε_2 remains small, we find that F_3 would be enhanced appreciably when ω satisfies $\varepsilon_1 = 0$. We call such a frequency the frequency of an eigen mode. An eigen mode exists in each frequency span between two adjacent cyclotron harmonics.

Thus an optimum frequency is expected at either a cyclotron frequency or a frequency of the eigen mode. However, Fig.5 also shows that ε_1 diverges at a cyclotron frequency; F_3 vanishes there. The singularities of F_2 and ε_1 at the cyclotron frequency cancel each other; it is thus expected that the product of F_2 and F_3 exhibits no singular behavior at the cyclotron frequency. Computational result of $F_2 \cdot F_3$, shown in Fig.6, indeed substantiates such an expectation; enhancement of the force should thus take place at the frequencies of the eigen modes. The critical difference between this conclusion and that based on Eq.(2) must be emphasized here; according to Eq.(2) the optimum frequency should take place at the cyclotron frequency.

Physically we may interpret the foregoing conclusion in the folloiwng way: For a given amplitude of the r.f. field, there is a tendency for an individual particle to experience an enhanced displacement at the cyclotron frequency. However such an enhanced response of the individual

particle also leads to a strong screening action of the plasma as a collection of such individual particles; the strength of the r.f. field inside the plasma is thereby reduced substantially. No remarkable phenomena are thus expected at the cyclotron frequency. On the other hand, an extensive enhancement of the r.f. field takes place at the frequency of an eigen mode determined from the equation, $\varepsilon_1 = 0$. Consequently, we may expect a drastic enhancement of the retarding force at such an optimum frequency.

Since ε_1 is known as a function of ω $k_\perp$, as can be seen from Eq.(39), $\varepsilon_1 = 0$ determines the dispersion relation of a collective mode in the plasma; the equation contains the density n and the magnetic field B as parameters. The wave number $k_\perp$ is fixed by the experimental boundary condition; we thus obtain two sets of solutions for $\varepsilon_1(\omega; n, B) = 0$ fixing either n or B. Figure 7 shows such a theoretical relation between the optimum frequency and the plasma density. It is particularly significant to note that the optimum frequency varies from the cyclotron frequency to twice that value, as the plasma density increases.

Figure 8 shows a similar relation between the optimum frequency and the magnetic field when the plasma density is fixed. Again it is important to note that the optimum frequency varies from the cyclotron frequency to twice that value as the strength of the field decreases. Thus the optimum frequency is expected somewhere between the cyclotron frequency and its second harmonic.

VI. LOSS FACTOR

We may attempt to use this concept of an r.f. plugging for a developmental study toward a thermonuclear reactor. For such a purpose it is important to have an estimate on the efficiency of such an r.f. plugging. Let us thus define the loss factor α as

$$\alpha = \frac{\text{(loss flux when r.f. field is applied)}}{\text{(loss flux when r.f. field is notapplied)}} \cdot \qquad (40)$$

A good plugging efficiency is obtained when α is small.

Based on Eq.(1), one would conclude that $\alpha = 0$ when $\omega = \omega_c$; an infinitely high potential barrier would prevent a particle from escaping from the system. Hatori and Watanabe[13] modified the individual-particle theory by taking into account a non-adiabatic behavior of charged particles. In the modified theory they classified the particles, according to the velocities, into two groups: adiabatic particles and non-adiabatic ones. With assumption that all the non-adiabatic particles would be lost from the system, they obtained a finite loss factor, consistent with experimental results.

In our theory the singularity at the cyclotron frequency has been removed by means of the dielectric screening action of the plasma. A new resonance structure appears at a frequency corresponding to the eigen mode of the plasma; even at such a frequency the loss factor remains finite. To calculate the loss factor, we integrate Eq.(35) along the z-axis; a finite potential ϕ is thereby obtained. With

the aid of the Boltzmann statistics, the loss factor is given by

$$\alpha = \exp\left(-\frac{\phi}{T}\right) . \qquad (41)$$

Equation (35) contains the local strength of the magnetic field through the cyclotron frequency ω_c. As a particle moves along a magnetic line of force, the local strength of the magnetic field changes; thus, ω_c is a function of z. Introducing a nondimensional variable $x = \omega_c(z)/\omega$, we rewrite Eq.(35) as

$$F = -\frac{q^2 E^2}{4 m \omega^2} \frac{1}{\varepsilon_1^2 + \varepsilon_2^2} \sum_{\nu=-\infty}^{\nu=\infty} \frac{x^2 I_\nu e^{-2}}{[(1-\nu x)^2 - x^2]^2} \frac{\nabla B}{B} , \qquad (42)$$

where we have from Eq.(39)

$$\varepsilon_1 = 1 - 2\frac{k_D^2}{k^2} \sum_{\nu=1}^{\infty} \frac{\nu^2 x^2}{1-\nu^2 x^2} I_\nu e^{-2} , \qquad (43)$$

$$\varepsilon_2 = \pi^{1/2} \frac{k_D^2}{k^2} \frac{k_\perp}{k_\parallel (2z)^{1/2} x} \times \sum_{\nu=-\infty}^{\nu=\infty} I_\nu e^{-2} \exp\left\{-\frac{k_\perp^2 (1-\nu x)^2}{2z\, k_\parallel^2 x^2}\right\} . \qquad (44)$$

Since we are interested in a high-density case so that $k_D^2/k^2 >> 1$, Eq.(43) may be simplified as

$$\varepsilon_1 = -\frac{k_D^2}{k^2} x \left(\frac{I_1(z)}{1-x} - \frac{2 I_2(z)}{1-2x}\right) e^{-z} \qquad (45)$$

The frequency of the eigen mode is then determined from the solution of $\varepsilon_1 = 0$ as

$$x = x_o \equiv \frac{I_1 + 2I_2}{2I_1 + 2I_2} \qquad (46)$$

For a small Larmor radius so that $z < 0.5$ we have $I_1 >> I_2$; consequently x_o approaches 1/2; the optimum frequency reduces to twice the cyclotron frequency in this limit.

As we are particularly interested in the vicinity of the optimum frequency, let us expand Eqs.(42)-(44) around $x = x_o$:

$$F = -\frac{q^2 E_o^2}{4m\omega^2} \frac{\nabla B}{B} \frac{F_2}{\varepsilon_1^2 + \varepsilon_2^2}, \qquad (47)$$

$$\varepsilon_1 = -\frac{k_D^2}{k^2} \frac{2x_o(x_o - x)}{(1-x_o)(1-2x_o)} I_1 e^{-z}, \qquad (48)$$

$$\varepsilon_2 = \pi^{1/2} \frac{k_D^2}{k^2} \frac{k_\perp}{k_\parallel x (2z)^{1/2}} I_2 e^{-z} \exp\left[-\frac{k_\perp^2 (1-2x_o)^2}{2k_\parallel^2 z x_o^2}\right], \qquad (49)$$

$$F_2 = \frac{I_1 e^{-z}}{4(1-2x_o)^2} \qquad (50)$$

After some rearrangement, we have from Eq.(47)

$$F = \frac{q^2 E^2}{4m\omega^2} \frac{\nabla B}{B} \left[\frac{k_o^2}{k^2} \frac{x_o}{1-x_o} 4 I_1 e^{-z}\right]^{-2} \times \frac{I_1 e^{-z}}{(x-x_o)^2 + \delta^2} \qquad (51)$$

$$\delta = \pi^{1/2} \frac{I_2}{I_1} \frac{(1-x_o)(1-2x_o)}{2k_\parallel x_o^2 (2z)^{1/2}} \exp\left[-\frac{k_\perp^2 (1-2x_o)^2}{2k_\parallel^2 z x_o}\right] \qquad (52)$$

Multiplying Eq.(51) by $(\omega/\nabla\omega_c)$ and integrating the resulting formula with respect to x, we obtain an expression for the potential as

$$\phi(x) = -\frac{q^2E^2}{4m\omega^2}\left(\frac{K^2}{k_D^2}\right)^2 \frac{(1-x_0)^2}{16\,x_0^3\,I_1\,e^{-2}} \times \frac{1}{\delta}\left[\frac{\pi}{2} + \tan^{-1}\frac{x-x_0}{\delta}\right] \qquad (53)$$

The value of $k_\perp$ may be estimated from a measurement of the standing waves inside the sheet plasma. The average Larmor radius ρ can also be obtained from an experimental determination of the ionic temperature. Hence, we may regard z as a fixed value; in our experimental condition, we find z = 0.4 to be an appropriate value. With the aid of these numerical considerations, we may simplify Eq.(53) as

$$\phi(x) = \frac{q^2E^2}{4m\omega^2}\left(\frac{\omega_c^2}{\omega_p^2}\right)^2 \frac{1}{\delta}\left[\frac{\pi}{2} + \tan^{-1}\frac{x-x_0}{\delta}\right] \qquad (54)$$

In the derivation of Eq.(54), we have ignored numerical factors of order unity. Carrying out a similar simplification, we find that the force F can be rewritten as

$$F(x) = -\frac{q^2E^2}{4m\omega^2}\left(\frac{\omega_c^2}{\omega_p^2}\right)^2 \frac{1}{\delta}\,\frac{\delta}{(x-x_0)^2+\delta^2}\,\frac{\nabla B}{B} \qquad (55)$$

Equation (54) can be factored into four parts: The first factor $q^2E^2/4m\omega^2$, having the dimension of a potential, represents a canonical strength of the potential involved in these problems. The second factor $(\omega_c^2/\omega_p^2)^2$ describes a

shielding effect. An increase of plasma density results in a decrease of the potential through ω_p^2, while the magnetic field acts to increase the potential. The third factor $1/\delta$, being large in magnitude, acts to ensure the potential large. The quantity δ arises from the calculation of

$$\delta = \left[\varepsilon_2 \cdot \left(\frac{\partial}{\partial x} \varepsilon_1 \right)^{-1} \right]_{x = x_o} \qquad (56)$$

It is thus closely related to the dissipation in the plasma. In fact, $1/\delta$ can be regarded as a Q-value when the plasma between the r.f. electrodes is looked upon as a resonance cavity. The last factor, $\{\pi/2 + \tan^{-1}[(x - x_o)/\delta]\}$, describes a sharp rise of the potential as x passes the point $x = x_o$.

Combining Eq.(54) with Eq.(41) we obtain the loss factor as

$$\alpha(x) = \exp\left\{ -\frac{1}{T} \frac{q^2 E^2}{4 m \omega^2} \left(\frac{\omega_c^2}{\omega_p^2} \right)^2 \frac{1}{\delta} \left[\frac{\pi}{2} + \tan^{-1} \frac{x - x_o}{\delta} \right] \right\} \qquad (57)$$

Going over to the limit of $x \to \infty$, we find the minimum value of the loss factor as

$$\alpha = \exp\left\{ -\frac{1}{T} \frac{q^2 E^2}{4 m \omega^2} \left(\frac{\omega_c^2}{\omega_p^2} \right)^2 \frac{\pi}{\delta} \right\} \qquad (58)$$

Let F_{ref} denote the flux reflected by this potential; it can be calculated as

$$F_{ref} = \alpha(x) - \alpha(\infty) \qquad (59)$$

In Fig.9, we depict schematic behavior of the force F, the potential ϕ and the reflected flux F_{ref}; Eq.(1) is also described by a dotted line.

We now wish to investigate the dependence of the loss factor on the intensity of the r.f. field and the density of the plasma. As Eq.(54) clearly indicates, the potential is proportional to the square of the field strength and is inversely proportional to the square of the plasma density. Figure 10 illustrates dependence of the loss factor on the field strength at a constant plasma density. Figure 11 shows the dependence of the loss factor on the plasma density at a fixed field strength. Plugging efficiency becomes worse with increase of the plasma density; an increase of the r.f. field strength can then compensate such a loss of plugging efficiency. Figure 12 shows the relation between the plasma density and the r.f. field strength to maintain a given value of the loss factor. These overall features of the interdependence among the physical parameters as demonstrated in the present study may be useful in constructing a scaling law associated with the concept of the r.f. confinement; one may attempt to scale up the size of the experiment with the aid of such a scaling law.

VII. COMPARISON WITH EXPERIMENTS

A. Optimum Frequency

Schematic diagram of the experiment is shown in Fig.13. A helium plasma is produced by a plasma source of the TPD

type[14] in one of the point cusps, and fed into the cusp container through a hole of the anode along magnetic lines of force. The density of the plasma ranges from 10^8 to 10^{11} cm^{-3} at the center of the container; the temperatures of the ions and electrons are almost the same and take on values between ten and twenty eV. Injected particles escape from the container through the open ends of the two point cusps and the line cusp, after several mirror reflections in the volume and non-adiabatic scattering at the center. The plasma forms a sheet at the line cusp, and its thickness is of the order of a Larmor radius. We call it the "sheet plasma". A pair of ring-shaped r.f. electrodes are set up, sandwitching the sheet plasma. We apply an r.f. voltage to the plasma through the electrodes; the loss flux of the ions is detected by a multigrid-type electrostatic analyzer at the end of the line cusp. In the presence of the r.f. voltage, the decrease of the ion losses is thereby detected.

Figure 14 shows the observed loss factor as a function of the r.f. frequency. The optimum frequency can be found at f = 1.9 MHz; this value is to be compared with the ion cyclotron frequency which is about 1.1 MHz. On the other hand, the optimum frequency calculated in the high-density limit, Eq.(46), is 2.1 MHz; this value is in satisfactory agreement with the experimental result. In order to describe the degree of plasma confinement achieved by the mechanism of the r.f. plugging, let us introduce the ratio β defined by

$$\beta = \frac{(\text{the plasma density at the center of the container when r.f. field is applied})}{(\text{the plasma density at the center of the container when r.f. field is not applied})}$$

The experimental values of β are also shown in Fig.14. At the optimum frequency where the loss of particles is minimized, the corresponding increase of the plasma density is observed.

When the magnetic field is varied, the optimum frequency varies accordingly as shown in Fig.15. The observed variation of the optimum frequency as a function of the magnetic field is then shown in Fig.16. This result is to be compared with the theoretical prediction of Fig.8; a qualitative agreement is indicated.

The optimum frequency is a function of the plsma density when the magnetic field is fixed. The loss rate of the particles is expected to be drastically minimized at a certain value of the plasma density when the r.f. frequency is kept constant. Let us call such a value the optimum density; a theoretical calculation of this density as a function of the frequency has been described in Fig.7.

In order to carry out an experiment pertaining to this effect, we create a decaying plasma by stopping the plasma injection; this can be done through short-circuiting the voltage applied between the cathode and the anode of the TPD type plasma source. The decay of the plasma density is observed at the center of the container by means of a double probe; the result is shown in Fig.17. The smooth decay curve in Fig.17 illustrates the feature in the absence

of the r.f. field; the wavy curve around it describes the change in the presence of the r.f. field. Clearly we here observe a suppressed rate of decay in the early stage. Generally, however, the place where the minimization of the decay rate takes place depends on the frequency. We may read out the values of the decay rate $-(1/n)(dn/dt)$ from Fig.17; we may thus plot the decay rate versus the density in Fig.18. The decay rate gives a measure of suppression of particle losses achieved by the r.f. plugging; the optimum density should thus correspond to minimum point of the curve in Fig.18. The optimum density determined in this way is plotted in Fig.19 as a function of the frequency of the r.f. field; the qualitative features exhibit a remarkable agreement with Fig.7.

B. Reflected Flux

Reflected flux is observed by means of a small multi-grid-type analyzer, movable radially along the sheet plasma in the line cusp as shown in Fig.20. Loss flux and reflected flux are shown in Fig.21; enhancement of the reflected flux and decrease of the loss flux take place at the same frequency. The spatial distribution of the reflected flux is revealed as one changes the position of the analyzer; the result is shown in Fig.22. Again, the main feature is consistently explained in terms of Fig.9.

C. Loss Factor

Equation (58) may provide a scaling law when the

concept of the r.f. plugging is applied to a thermonuclear device. A salient feature of the prediction is that the plugging becomes less effective when the plasma density is increased; the plugging efficiency may be recovered as one increases the r.f. voltage applied to the plasma.

The dependence of the loss factor α on the r.f. field and the plasma density is also investigated experimentally.[8,9] Figure 23 shows the loss factor at the optimum frequency as a function of the strength of the r.f. field. This result, when it is compared with the theoretical calculation of Fig.10, shows a good qualitative agreement. Empirical relation between the loss factor and the r.f. field strength may be expressed as $\alpha = \exp(-AE^x)$ with $x = 1.4$; this result differs slightly from the theoretical value $x = 2$ in Eq.(58). Recent study indicates that this difference could be accounted for in terms of the effect of charge separation created around the r.f. electrodes.

The density dependence of the loss factor is also obtained experimentally. Density of the plasma is varied from 10^{10} to 2×10^{11} cm^{-3} by changing the discharge current of the plasma source. Figure 24 illustrates such a dependence of the loss factor; it can be compared satisfactorily with the theoretical result of Fig.11. Parameters in the figure represent the intensities of the r.f. field; an improved loss factor is obtained through application of an intense r.f. field.

Figure 25 shows the relation between the plamsa density and the intensity of the r.f. field when the value of the

loss factor is kept constant; an empirical relation, E/n = const. thereby obtained, is a result in fact predicted in Eq.(58).

VIII. CONCLUSION

We have thus developed a theory of the r.f. plugging with inclusion of the collective effects brought about by the dynamic screening action of the plasma. The detailed features of the theoretical predictions are compared with experimental results, demonstrating a satisfactory agreement between them.

ACKNOWLEDGEMENT

The authors would like to express their gratitude to Dr. K. Takayama, Dr. T. Watanabe, and Dr. T. Hatori for helpful discussions, and to Mmes. E. Hosokawa and M. Watari for their typewriting.

REFERENCES

1. D. G. Dow and R. C. Knechetli, J. Electron. Contr. 7, 316 (1959)
2. T. Consoli, *Proc. Third Intern. Conf. on Plasma Physics and Controlled Nuclear Fusion Research*, Vol.2 (IAEA, Vienna, 1969) p.361
3. S. Miyake, T. Sato and K. Takayama, J. Phys. Soc. Japan 27, 1611 (1969)
4. T. Sato, S. Miyake, T. Watari, Y. Kubota and K. Takayama, J. Phys. Soc. Japan 28, 808 (1970)
5. T. Sato, S. Miyake, T. Watari, T. Watanabe, S. Hiroe, K. Takayama and K. Husimi, *Proc. Symp on Feedback and Dynamic Control of Plasmas* (American Institute of Physics, New York, 1970) p.310
6. S. Miyake, T. Sato and K. Takayama, J. Phys. Soc. Japan 29, 769 (1970)
7. S. Miyake, T. Sato, K. Takayama, T. Watari, S. Hiroe, T. Watanabe and K. Husimi, J. Phys. Soc. Japan 31, 265 (1971)
8. T. Watari, S. Hiroe, T. Watanabe, T. Hatori, T. Sato, K. Takayama and K. Husimi, *Proc. the Fifth European Conf. on Nuclear Fusion and Plasma Physics* (Grenoble, August 1972) p.104
9. S. Hiroe, T. Watari, T. Sato, T. Watanabe, T. Hatori, and K. Takayama, Ann. Rev. of Inst. Plasma Phys., Nagoya Univ., Nagoya, Japan (1971-1972) p.54

10. H. Motz and C. J. H. Watson, *Advances in Electronics*, Vol.23 (Acedemic Press, New York, 1967) p.153

11. S. Ichimaru, *Basic Principles of Plasma Physics* (W. A. Benjamin Inc., Reading, Mass., 1973) Chap.10

12. T. Watanabe and T. Hatori, Research Reports of the Inst. Plasma Phys., Nagoya Univ., Nagoya, Japan, IPPJ-132 and IPPJ-133 (1972)

13. T. Watanabe and T. Hatori, Ann. Rev. of the Inst. Plasma Phys., Nagoya Univ., Nagoya, Japan (1970-1971) p.172

14. K. Takayama, M. Otsuka, Y. Tanaka, K. Ishii and Y. Kubota, *Proc. Eighth Intern. Conf. on Phenomena in Ionized Gases* (IAEA, Vienna, 1967) p.551

FIGURE CAPTIONS

Fig.1. Mechanism of the r.f. plugging.

Fig.2. Coordinates.

Fig.3. The electrodes and the plasma.

Fig.4. Graph of F_2; $k_{\parallel} = 0.5$, $k_{\perp} = 1.5$, $k_D = 3.35$, and $Z = 0.5$ are assumed in the computation.

Fig.5. Graph of ε_1; the computation is made with the same condition as Fig.4.

Fig.6. Graph of $F_2 \cdot F_3$; the computation is made with the same condition as Fig.4.

Fig.7. The optimum frequency versus the plasma density; $B = 1.4$ kG, $T_e = 10$ eV, and $Z = 0.4$ are assumed in the computation.

Fig.8. The optimum frequency versus the magnetic field; $Z = 0.4$ and $n = 10^8$ cm^{-3} are assumed in the computation.

Fig.9. Schematic behavior of repelling force (a), potential (b), and reflected flux (c); the dashed line represents the potential obtained from the individual-particle model of Eq.(2).

Fig.10. Loss factor versus the r.f. field.

Fig.11. Loss factor versus the plasma density; the parameter $A = \frac{e^2E^2}{4m\omega^2} \frac{1}{T} \frac{\pi}{\delta}$.

Fig.12. The relation between the plasma density and the r.f. field at a constant loss factor; $B = 1400$ G is assumed.

Fig.13. Schematic diagram of the experimental apparatus.

Fig.14. The frequency dependence of α and β. The solid line expresses α and the dotted line β.

Fig.15. The variation of the optimum frequency with the magnetic field.

Fig.16. The optimum frequency versus the magnetic field. The cyclotron frequency cannot be determined uniquely since the magnetic field varies under the electrodes. The dashed regions in the figure show the ranges resulting from such an uncertainty.

Fig.17. Decay curves of the plasma density at the center of the container with the without the r.f. field (see the text). The scele factor of the abscissa is 100 μsec/div.

Fig.18. Decay rate versus the plasma density.

Fig.19. The optimum frequency versus the plasma density. The shaded regions in the figure show uncertainty in the cyclotron frequency.

Fig.20. Experimental setup for the measurement of the spatial distribution of the reflected flux.

Fig.21. Reflected flux and loss flux as functions of the frequency of the r.f. field.

Fig.22. Spatial distribution of the reflected flux.

Fig.23. Loss factor versus the r.f. field.

Fig.24. Loss factor versus the plasma density. E_o represents the strength of the r.f. field.

Fig.25. The relation between the plasma density and the r.f. field at a constant loss factor.

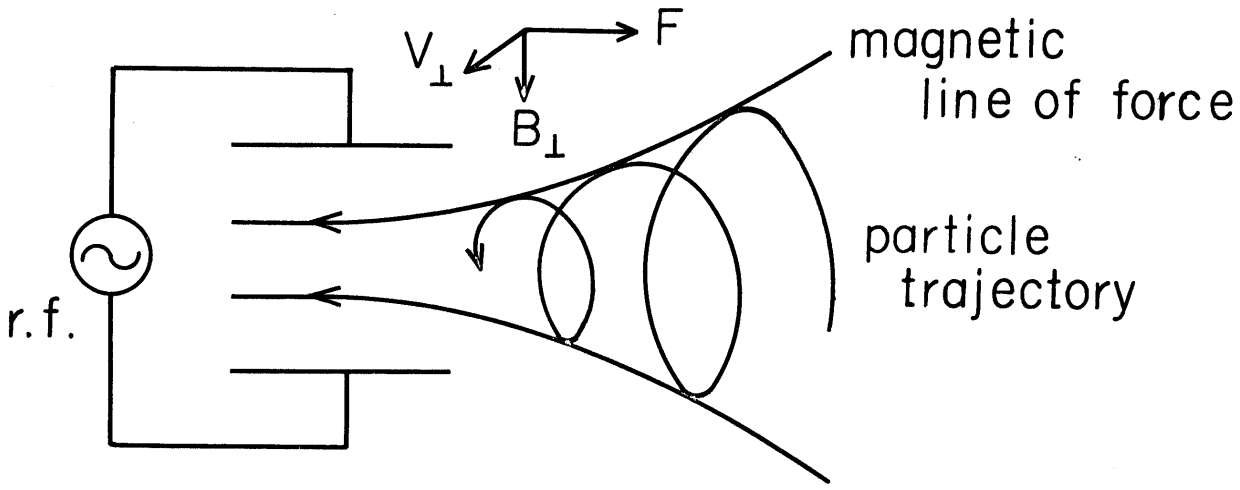
F
$V_\perp$
$B_\perp$
magnetic
line of force
particle
trajectory
r.f.

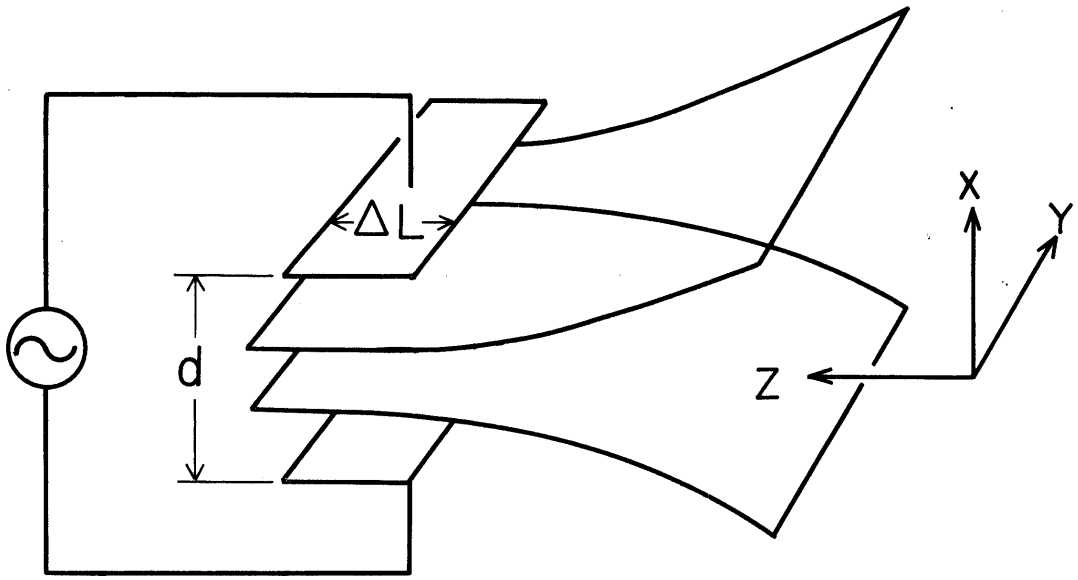
ΔL
d
X
Y
Z

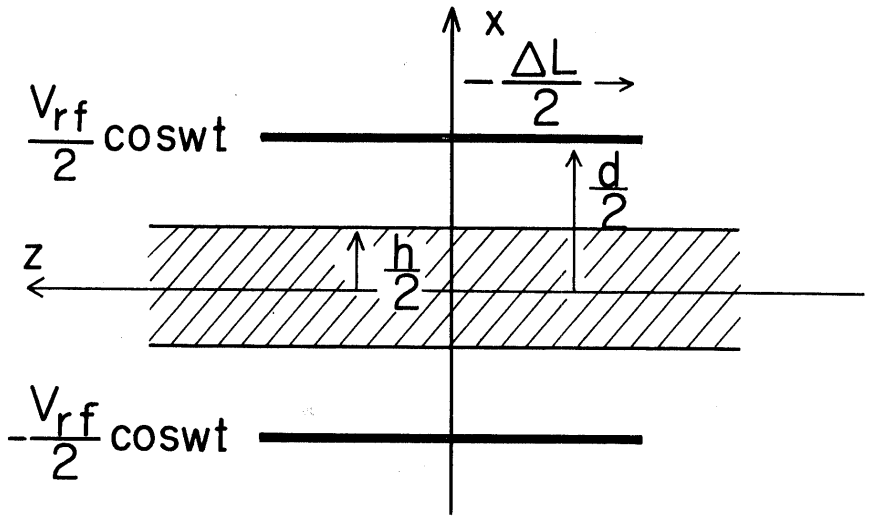
x
$-\frac{\Delta L}{2}$
$\frac{V_{rf}}{2}\cos\omega t$
$\frac{d}{2}$
z
$\frac{h}{2}$
$-\frac{V_{rf}}{2}\cos\omega t$

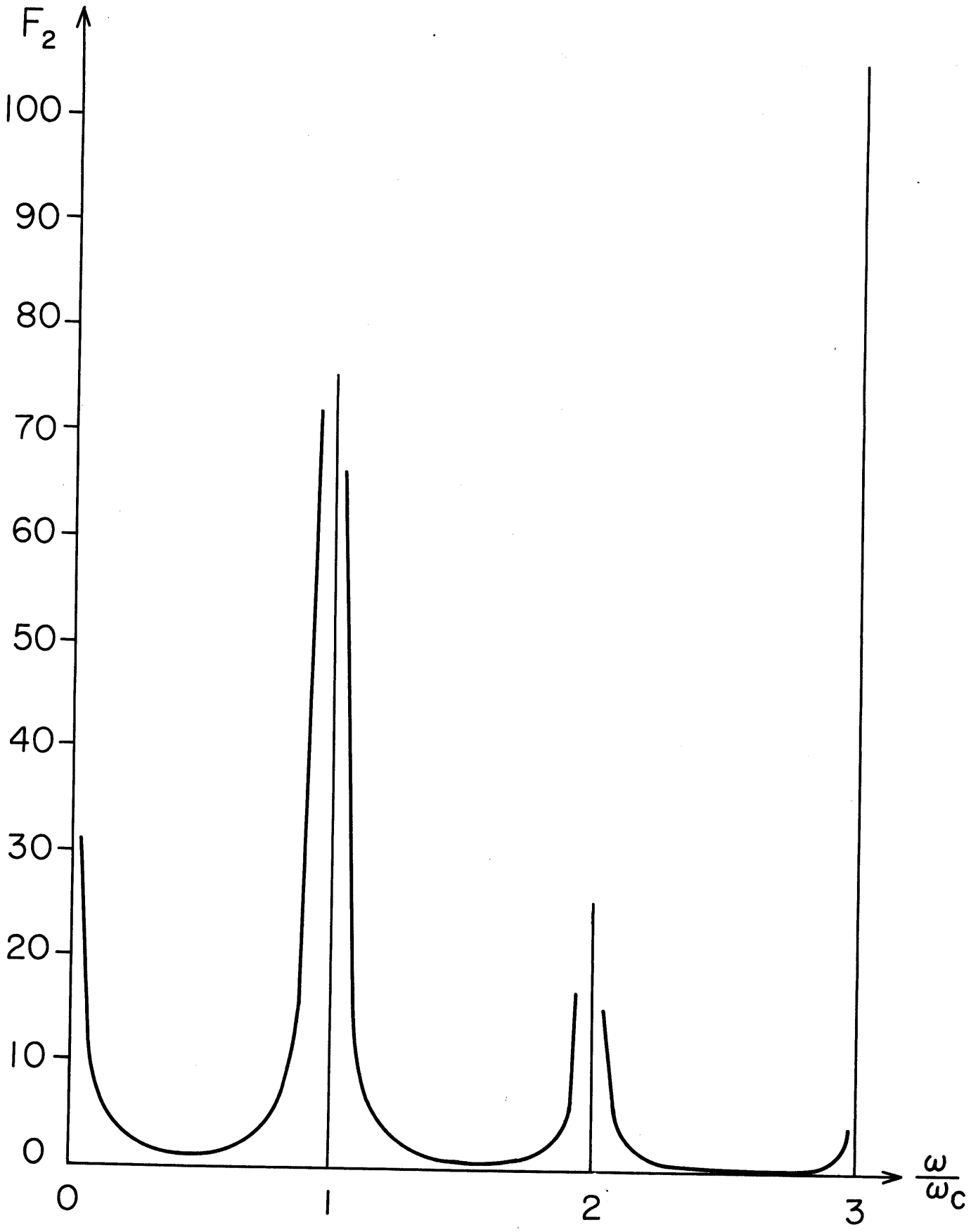
F_2
100
90
80
70
60
50
40
30
20
10
0
0
1
2
3
$\frac{\omega}{\omega_c}$

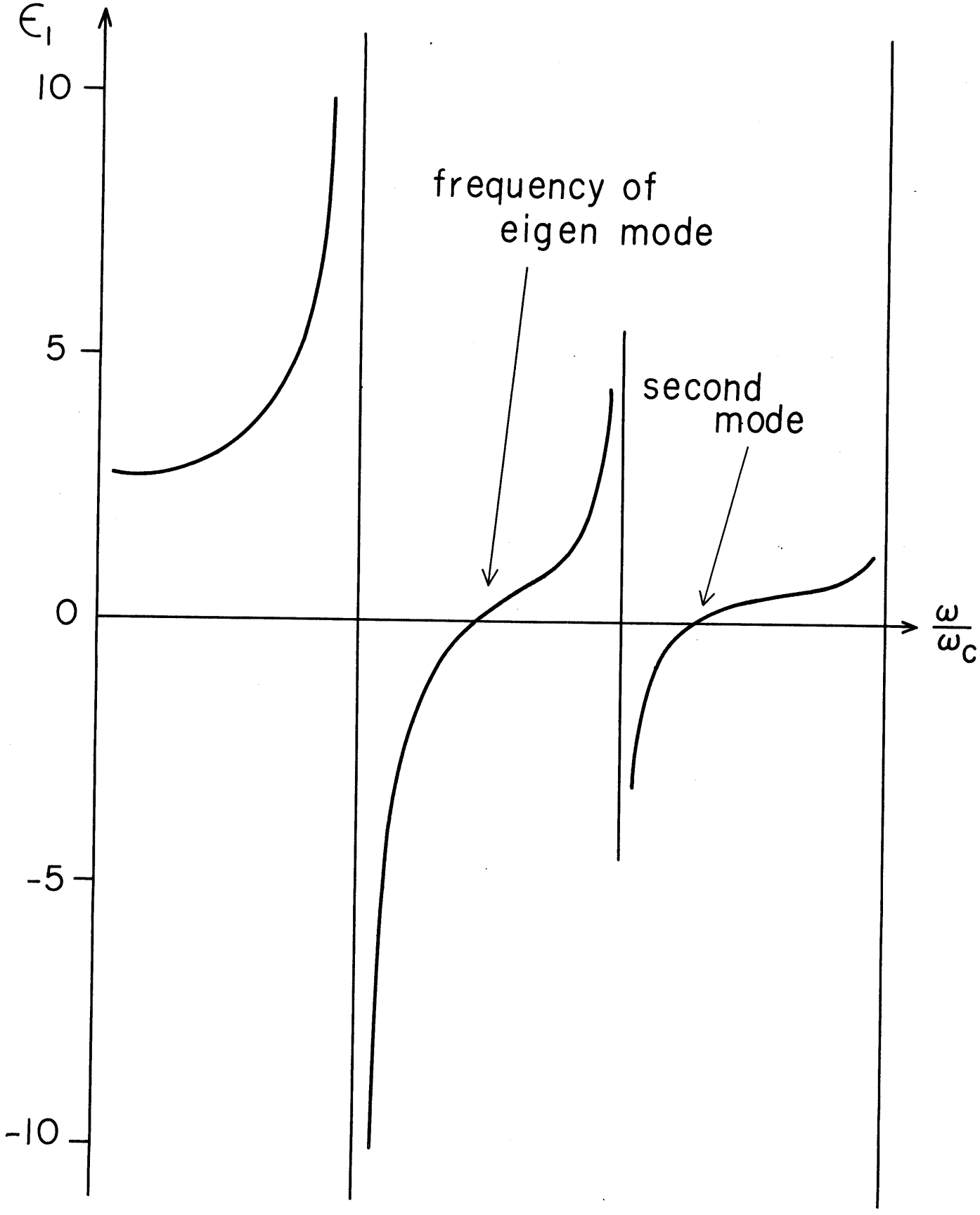
ϵ_1
10
5
0
-5
-10
frequency of
eigen mode
second
mode
$\frac{\omega}{\omega_c}$

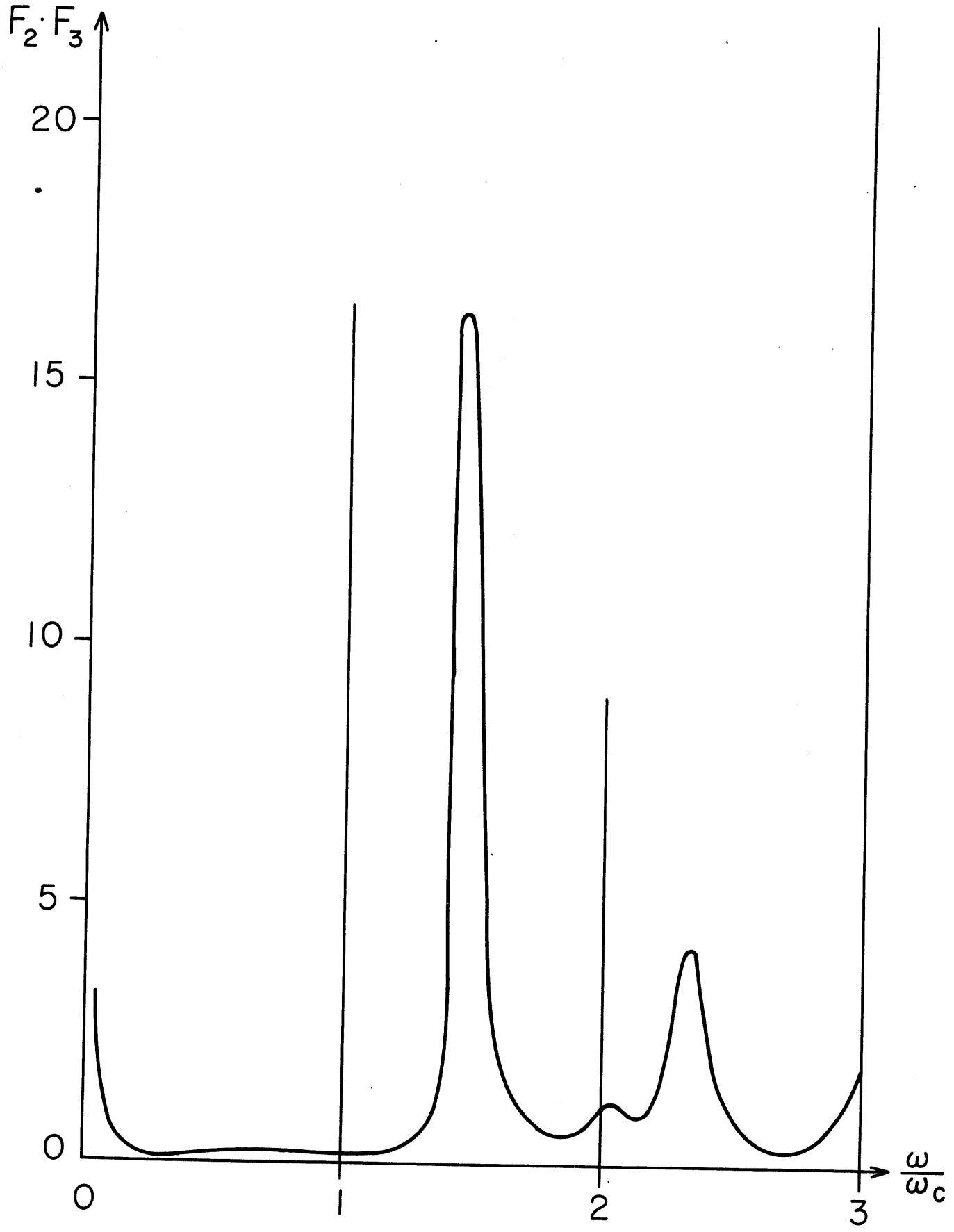
F2·F3
20
15
10
5
0
0
1
2
3
ω/ωc

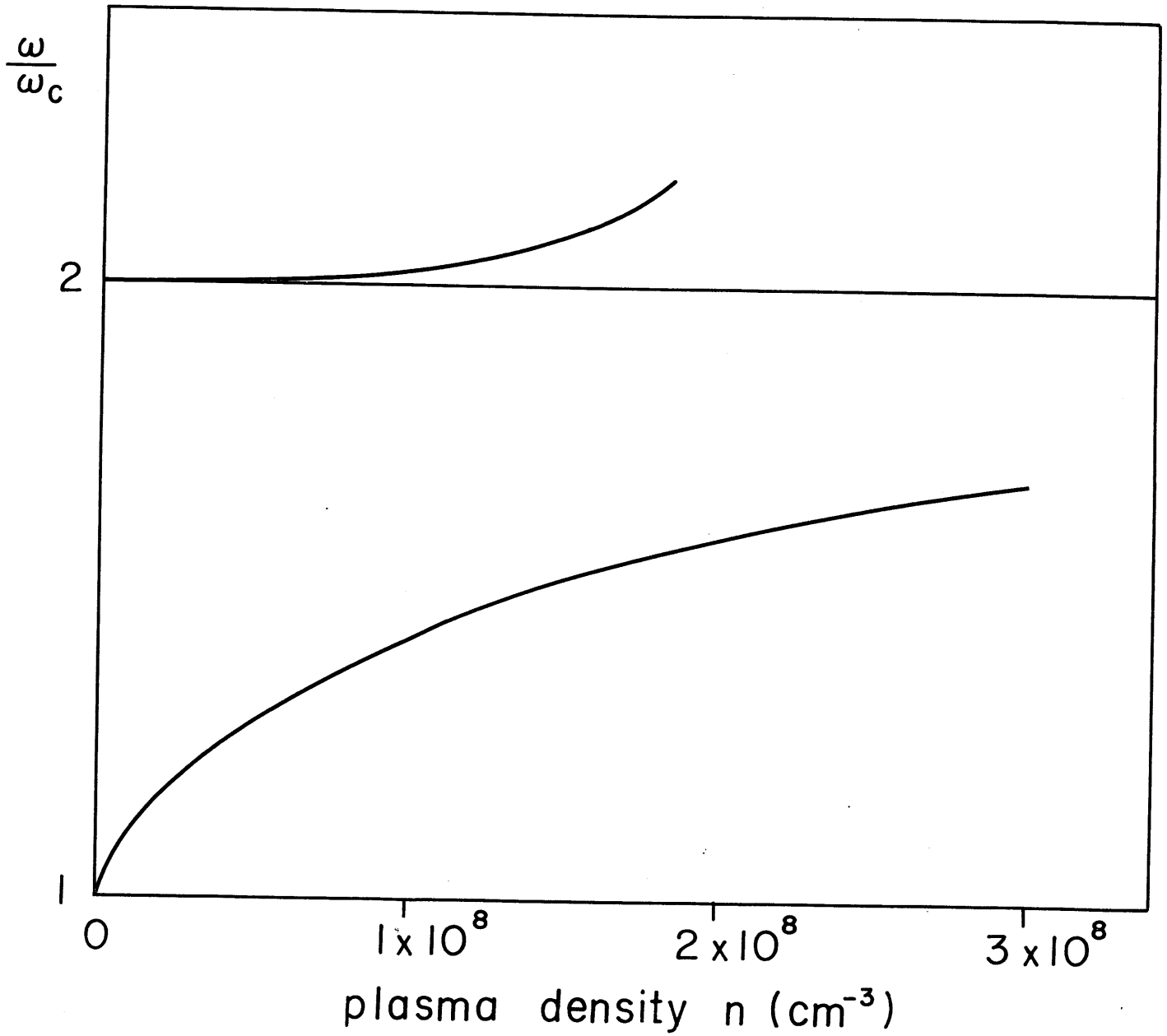
ω/ω_c
2
1
0
1 x 10^8
2 x 10^8
3 x 10^8
plasma density n (cm^-3)

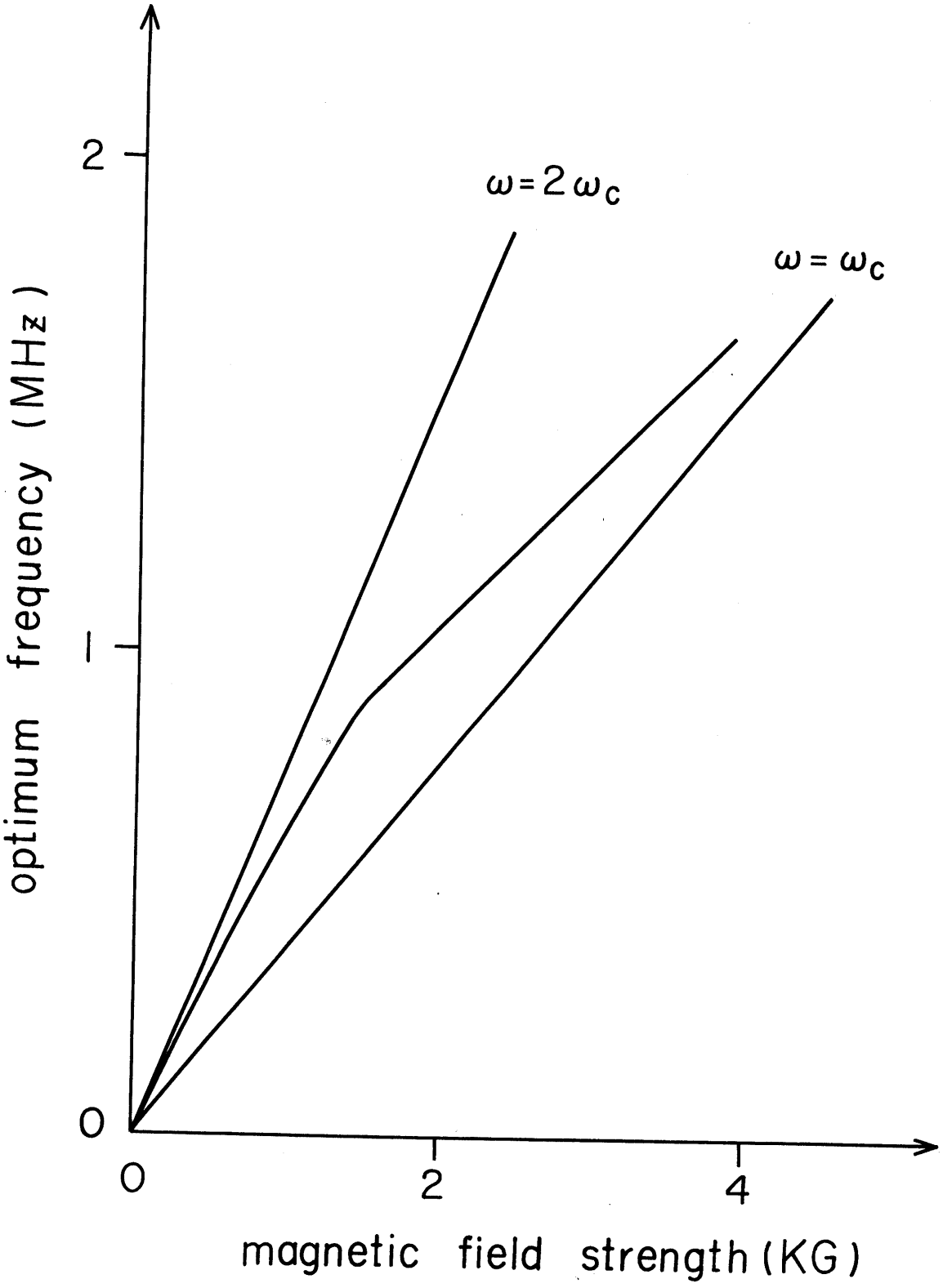
optimum frequency (MHz)
2
1
0
0
2
4
magnetic field strength (KG)
ω = 2 ω_c
ω = ω_c

$$F = \frac{e^2 E^2}{4m\omega^2}\left(\frac{\omega_c^2}{\omega_p^2}\right)^2 \frac{1}{\delta}\,\frac{\delta}{(x-x_0)^2+\delta^2}\,\frac{\Delta B}{B}$$

$$\phi = \frac{e^2 E^2}{4m\omega^2}\left(\frac{\omega_c^2}{\omega_p^2}\right)^2 \frac{1}{\delta}\left[\frac{\pi}{2} + \tan^{-1}\frac{x-x_0}{\delta}\right]$$

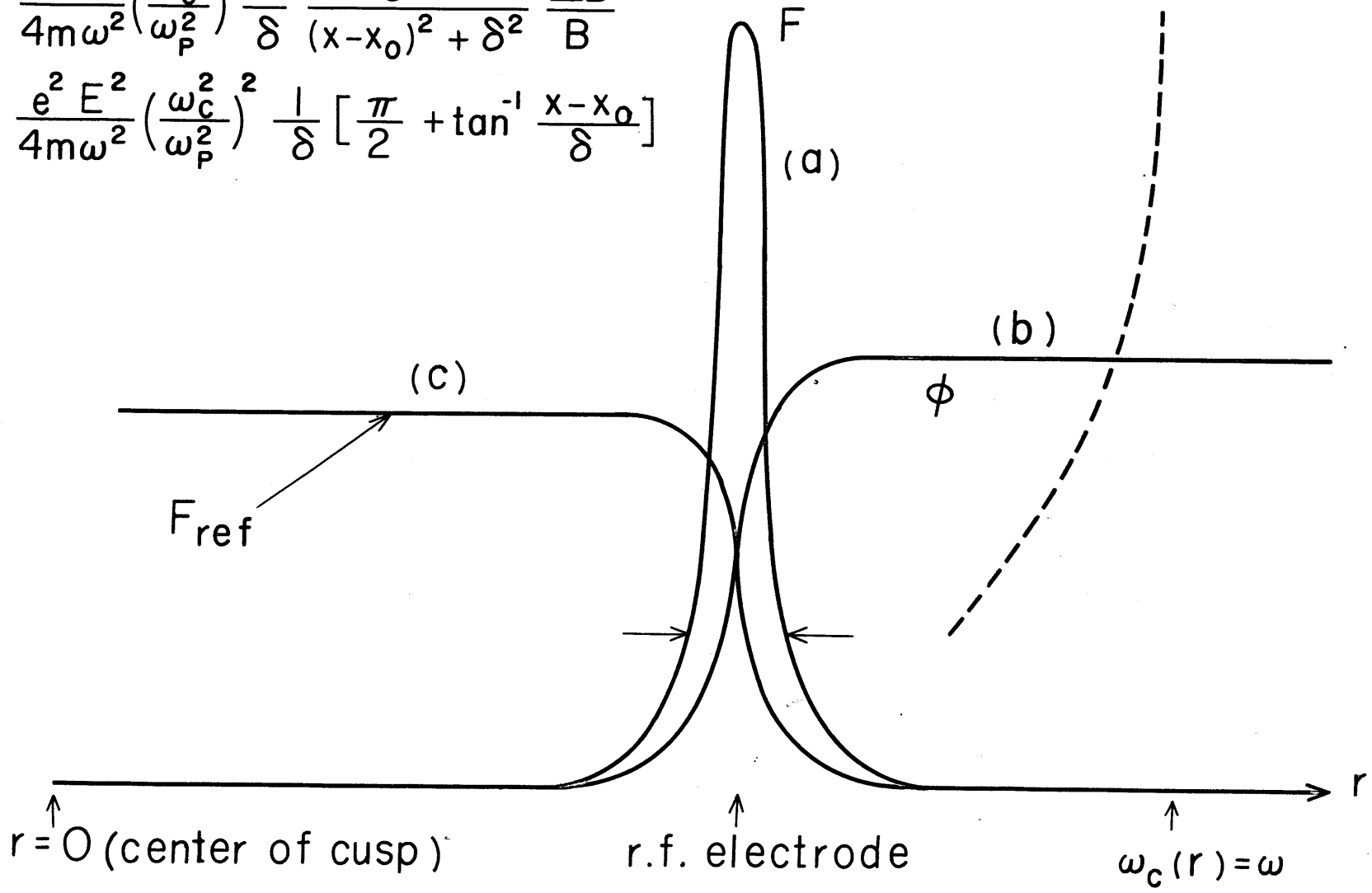

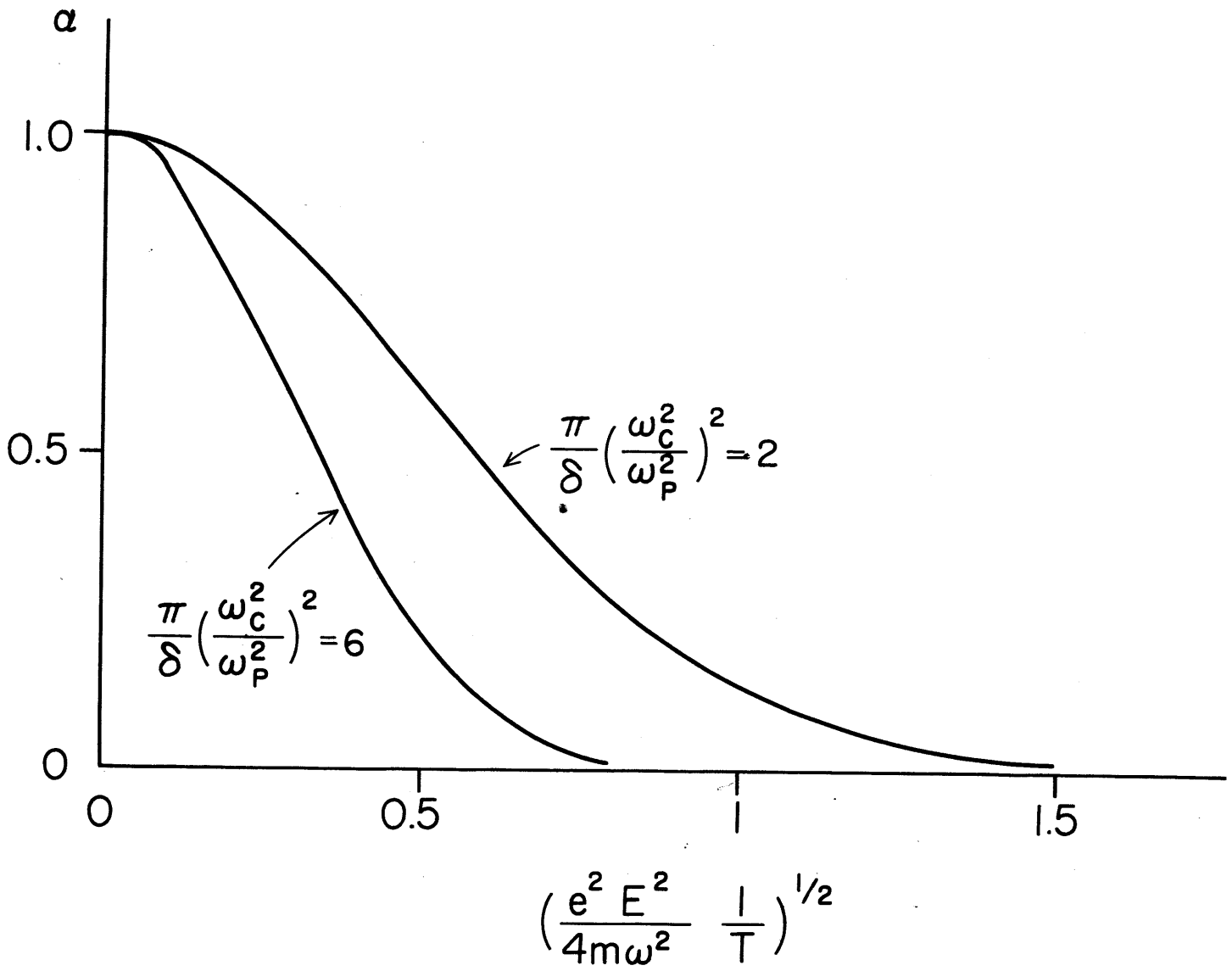
α
1.0
0.5
0
0
0.5
1
1.5
$\frac{\pi}{\delta}\left(\frac{\omega_c^2}{\omega_p^2}\right)^2 = 2$
$\frac{\pi}{\delta}\left(\frac{\omega_c^2}{\omega_p^2}\right)^2 = 6$
$\left(\frac{e^2 E^2}{4m\omega^2}\ \frac{1}{T}\right)^{1/2}$

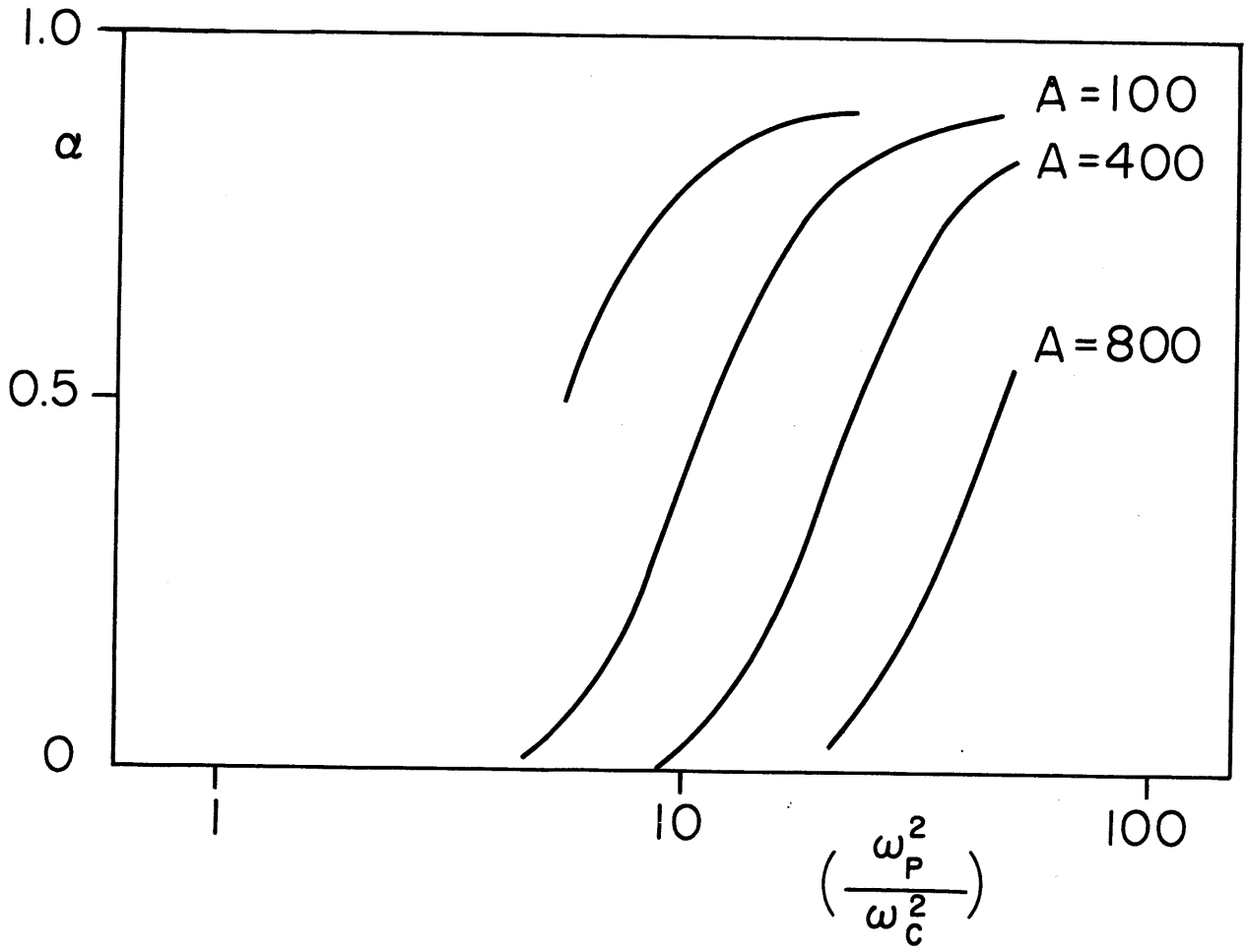
1.0
α
0.5
0
A=100
A=400
A=800
1
10
100
$\left(\frac{\omega_P^2}{\omega_c^2}\right)$

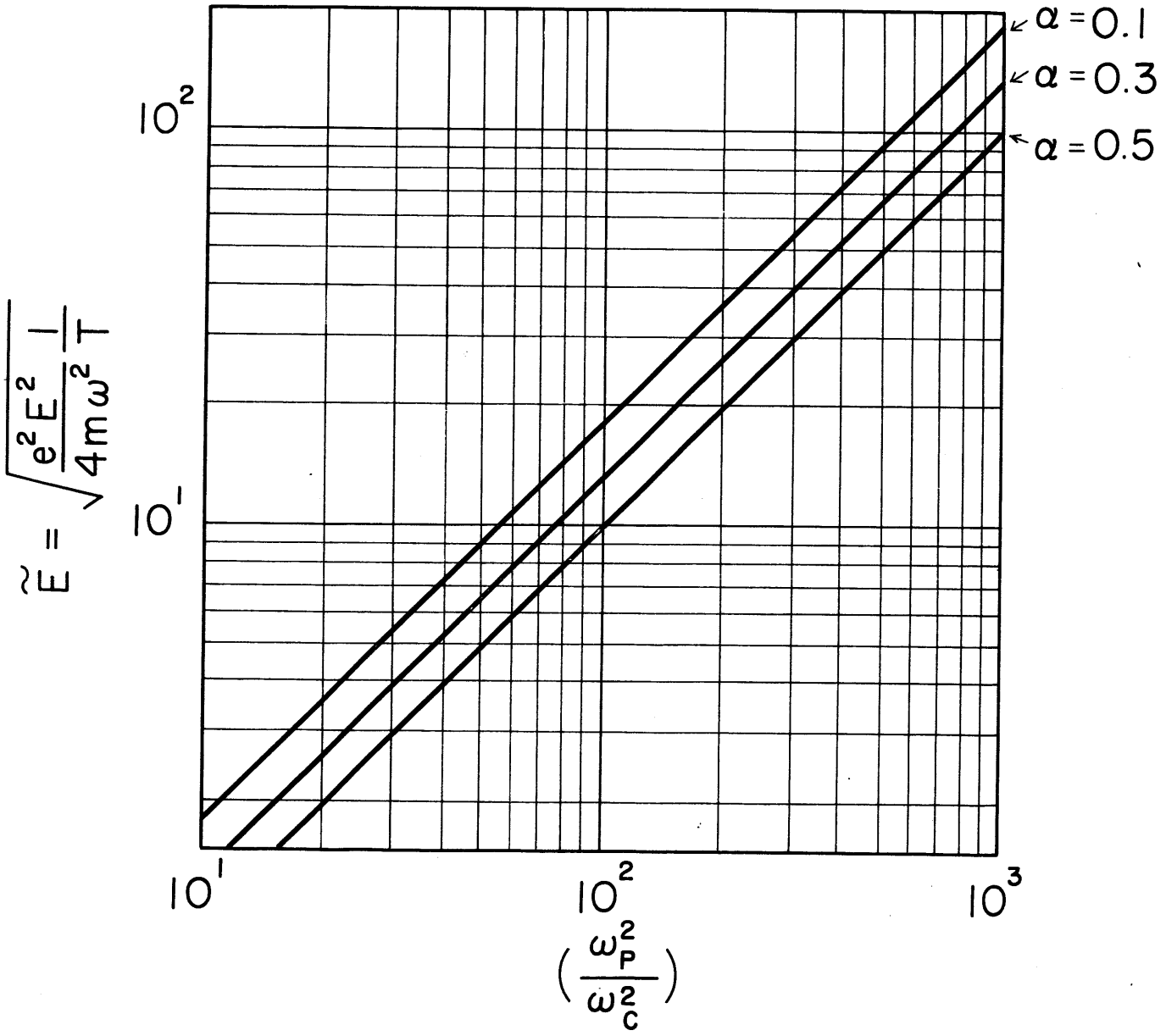
$\alpha = 0.1$
$\alpha = 0.3$
$\alpha = 0.5$
10^2
10^1
10^1
10^2
10^3
$\tilde{E} = \sqrt{\frac{e^2E^2}{4m\omega^2}\frac{1}{T}}$
$\left(\frac{\omega_p^2}{\omega_c^2}\right)$

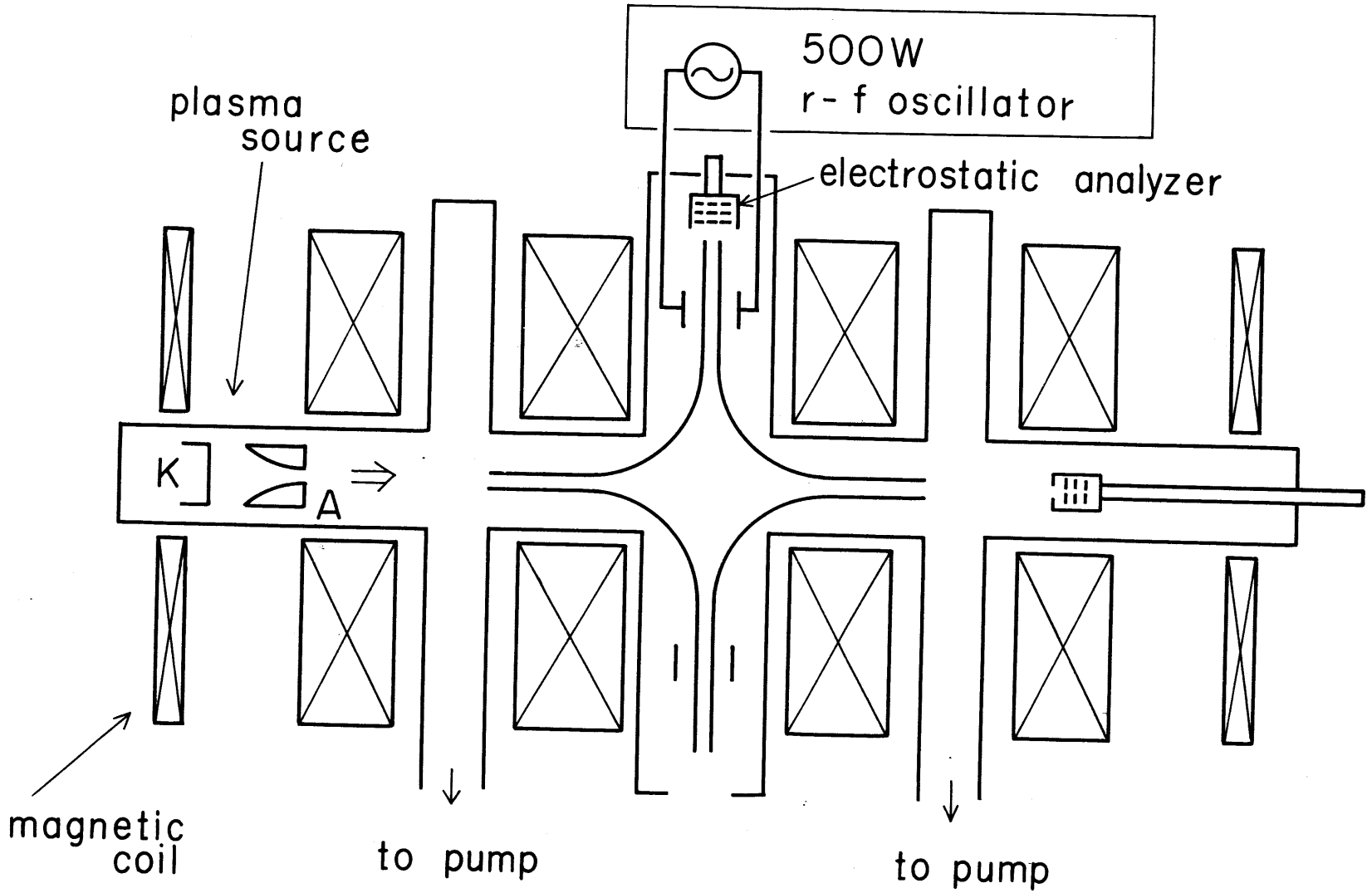
500W
r-f oscillator
plasma
source
electrostatic analyzer
K
A
magnetic
coil
to pump
to pump

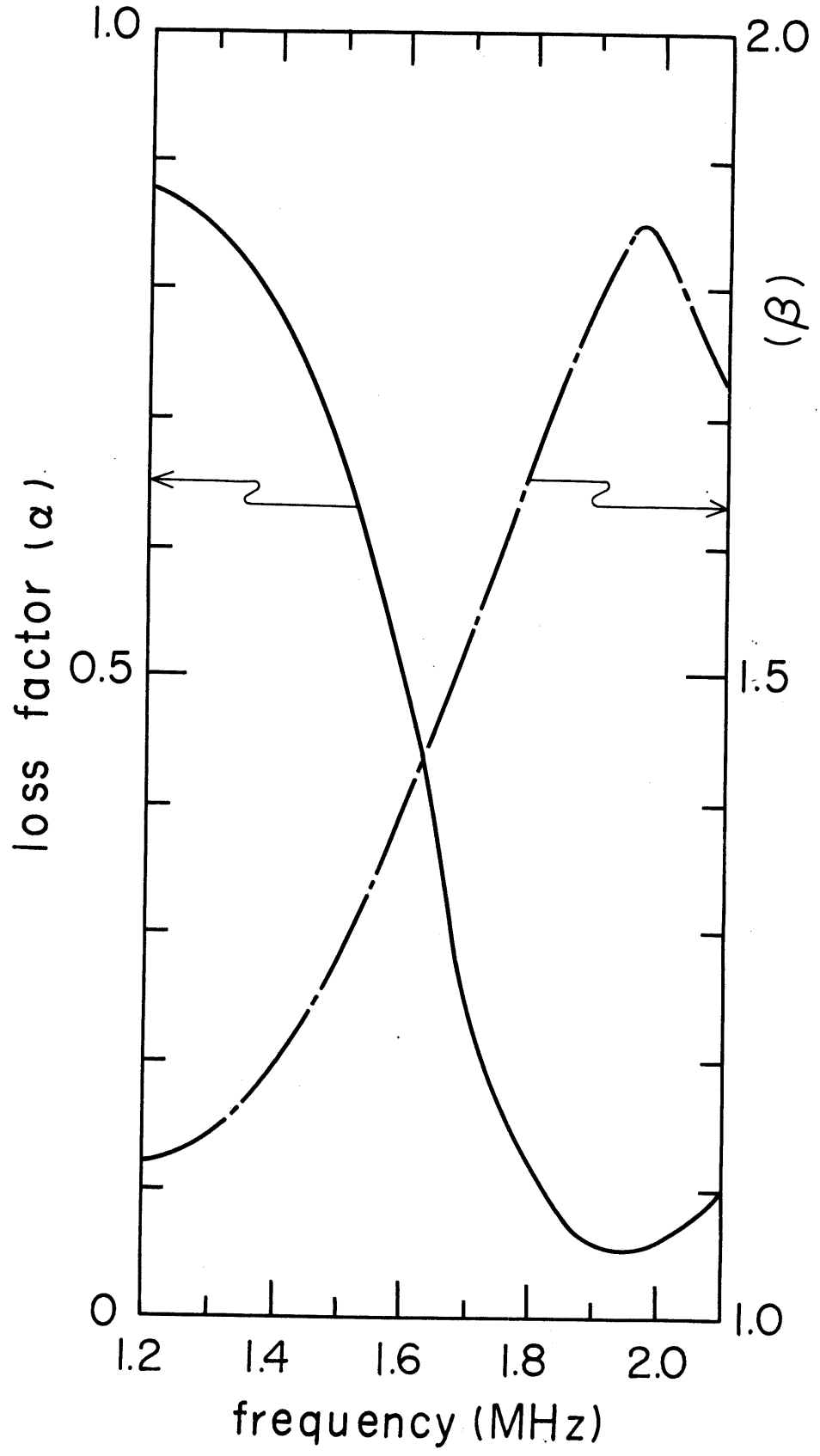
1.0
2.0
0.5
1.5
0
1.0
loss factor (α)
(β)
1.2
1.4
1.6
1.8
2.0
frequency (MHz)

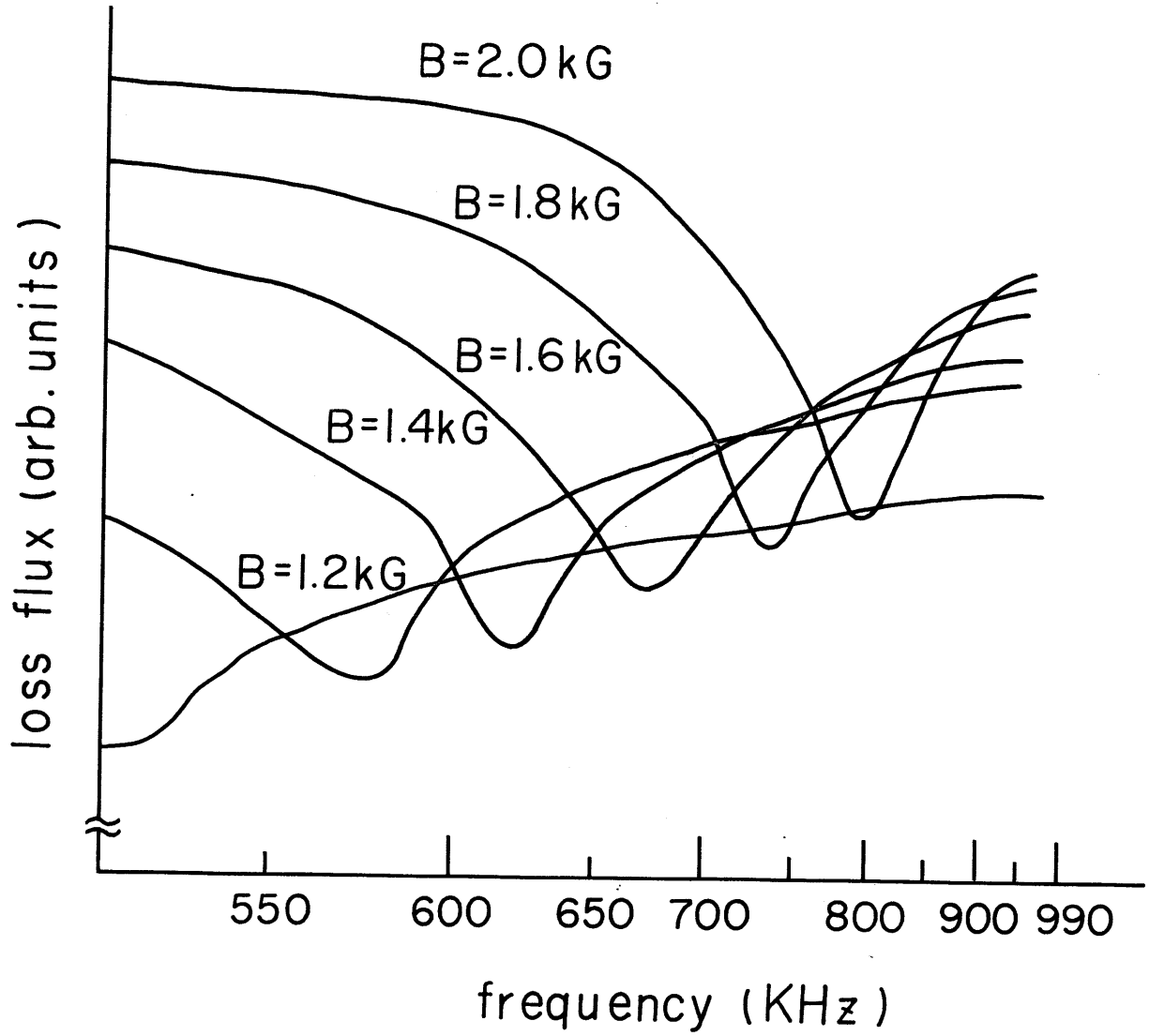
B=2.0kG
B=1.8kG
B=1.6kG
B=1.4kG
B=1.2kG
loss flux (arb. units)
550
600
650
700
800
900
990
frequency (KHz)

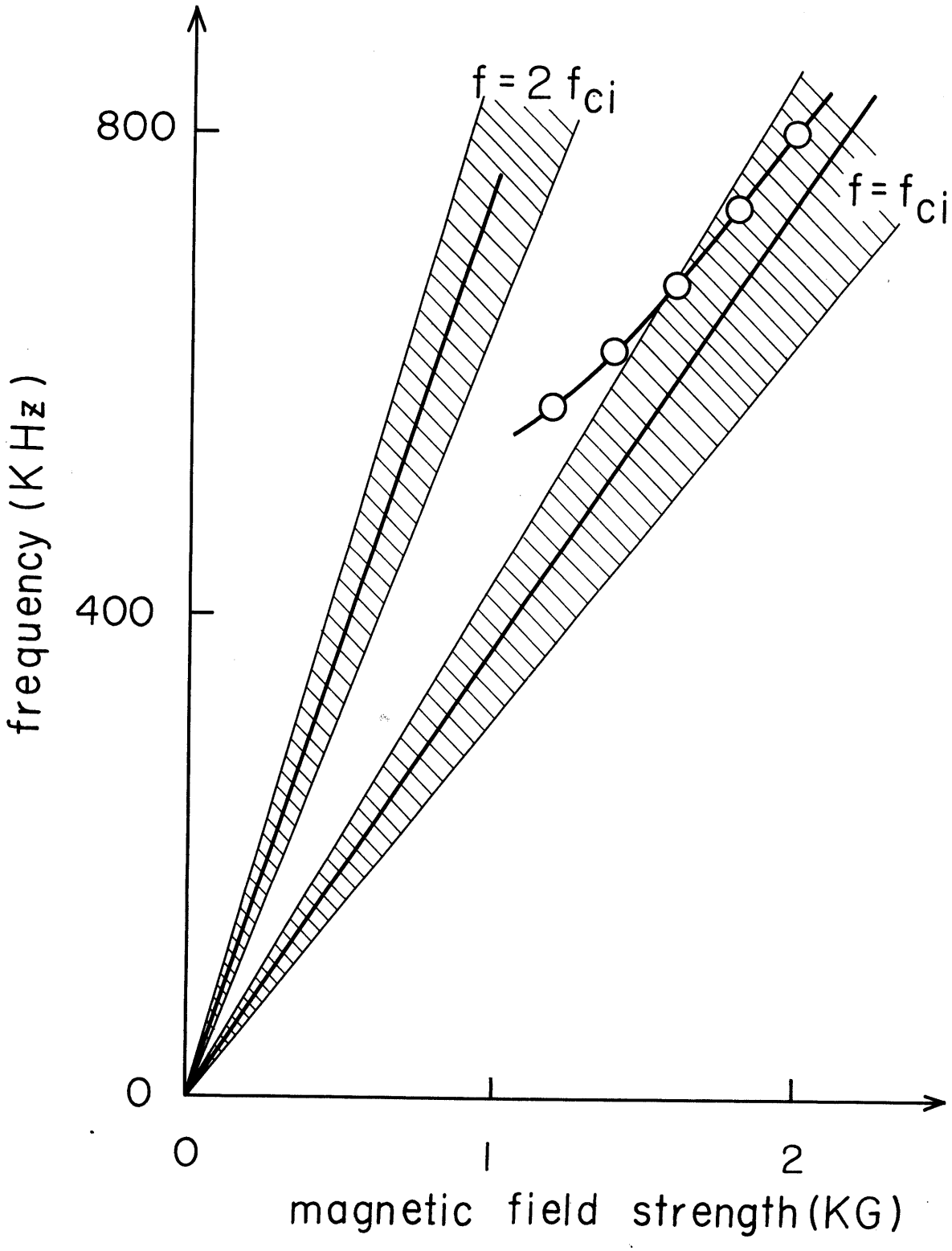
f = 2 fci
f = fci
800
400
0
frequency (KHz)
0
1
2
magnetic field strength (KG)

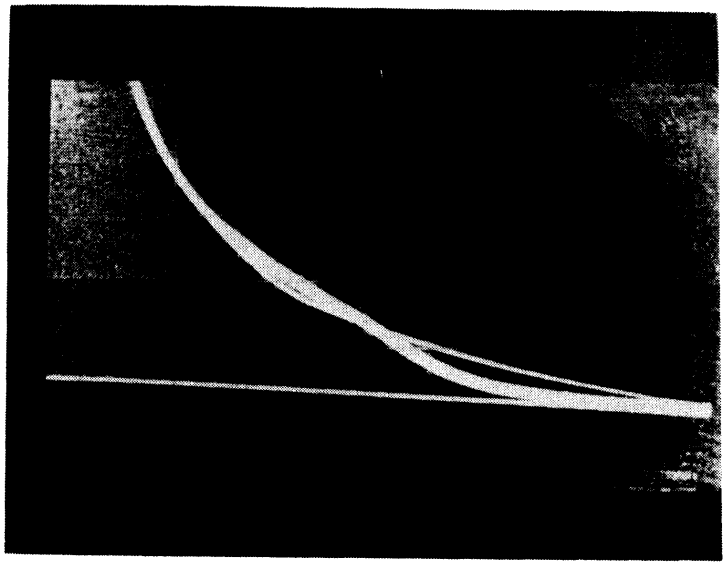

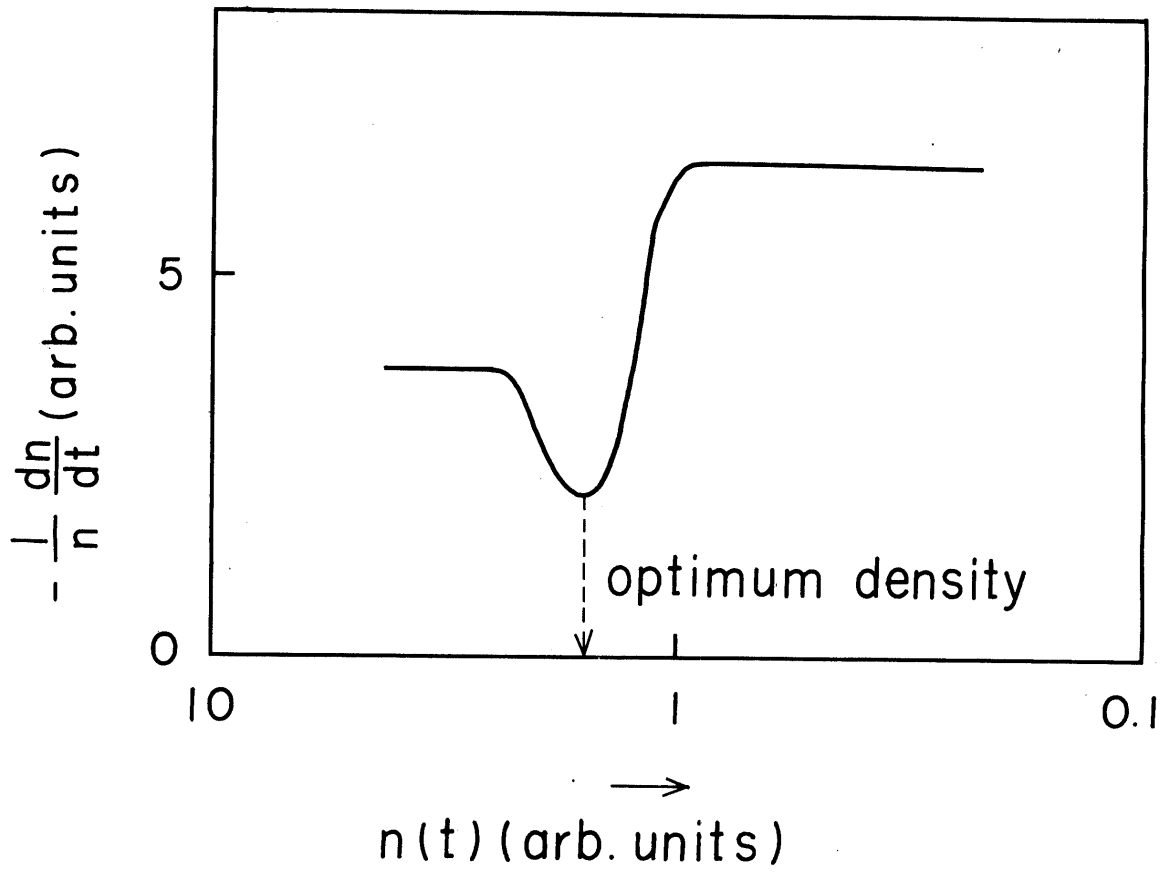
$-\frac{1}{n}\frac{dn}{dt}$ (arb. units)
5
0
optimum density
10
1
0.1
n(t) (arb. units)

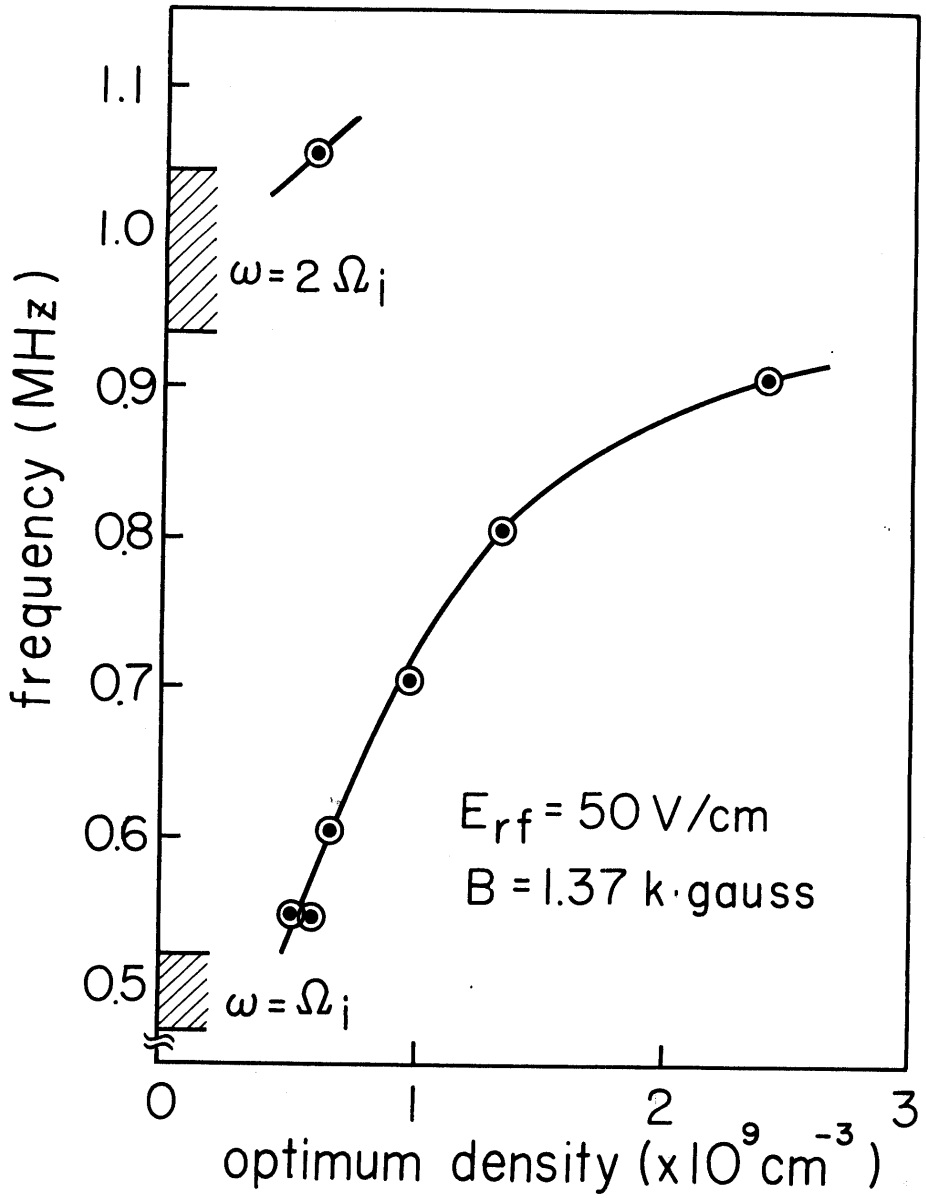
1.1
1.0
0.9
0.8
0.7
0.6
0.5
frequency (MHz)
ω = 2 Ω_i
ω = Ω_i
E_rf = 50 V/cm
B = 1.37 k·gauss
0
1
2
3
optimum density (x10^9 cm^-3)

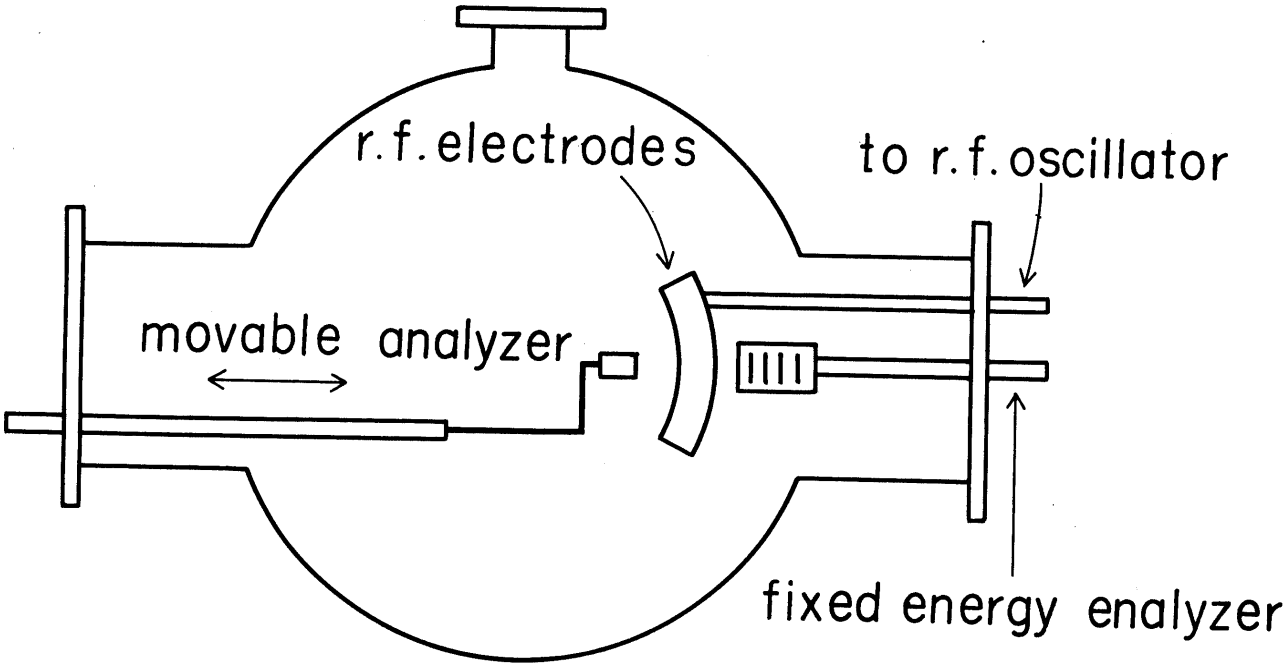
r.f. electrodes
to r.f. oscillator
movable analyzer
fixed energy enalyzer

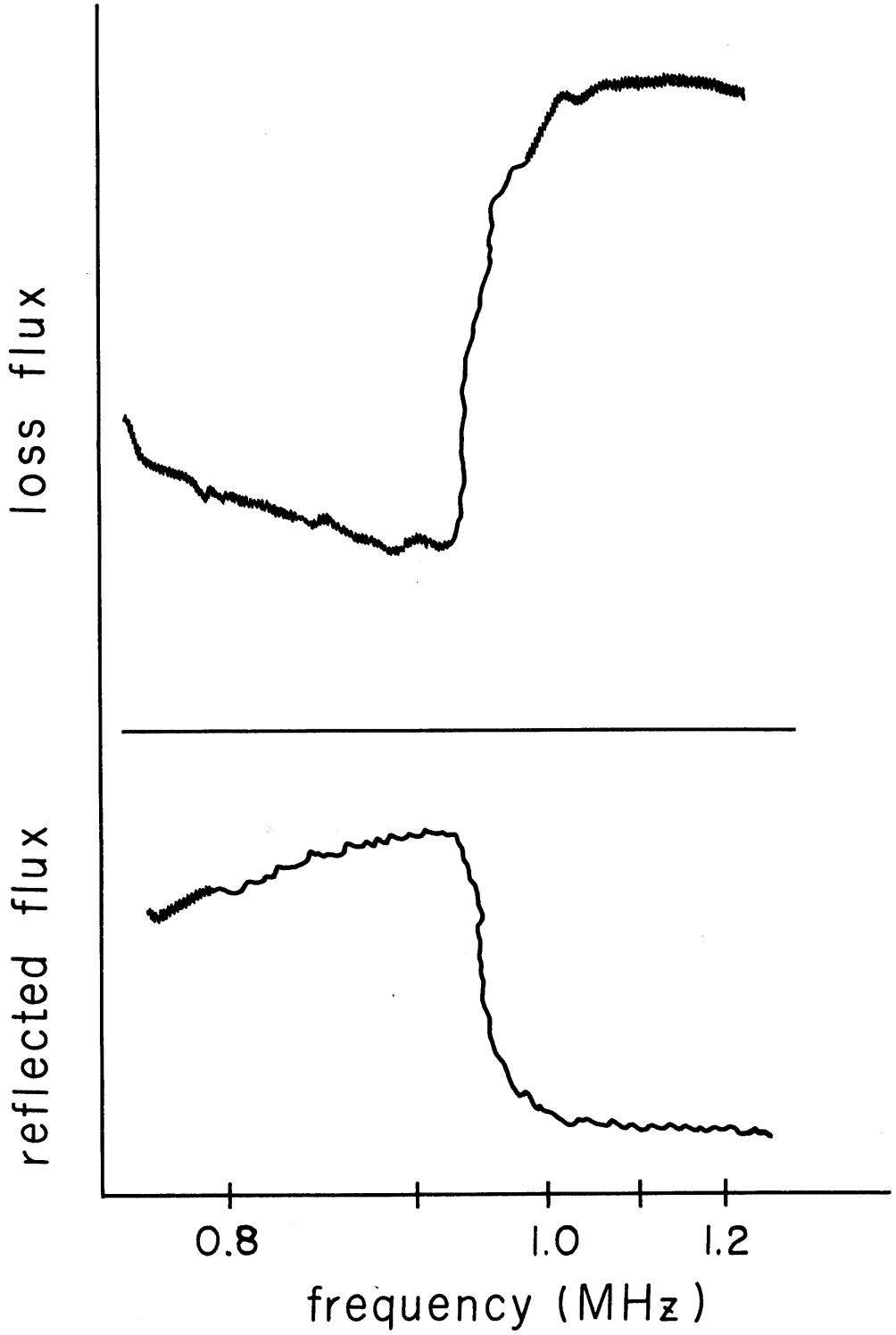
loss flux
reflected flux
0.8
1.0
1.2
frequency (MHz)

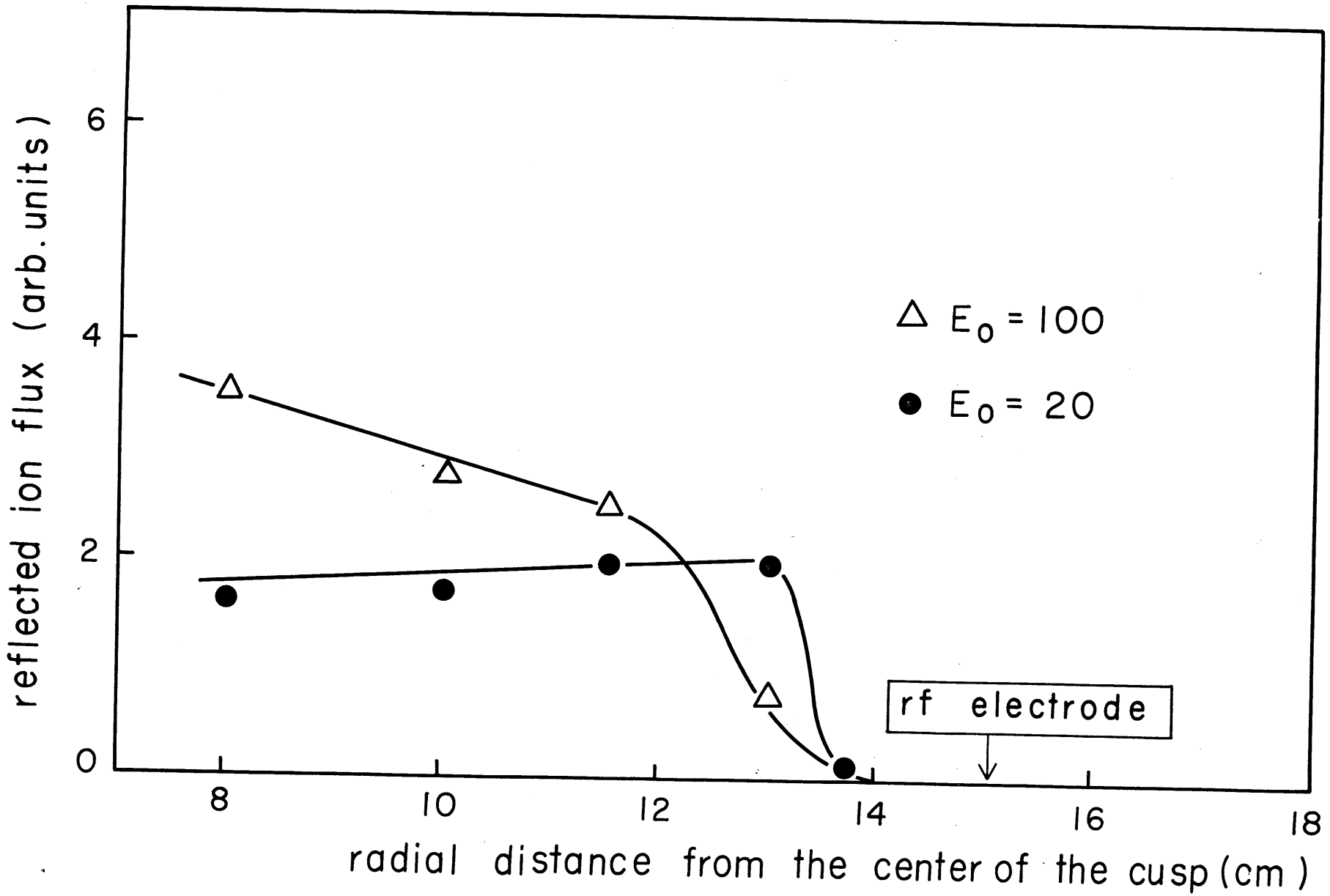
reflected ion flux (arb. units)
6
4
2
0
8
10
12
14
16
18
radial distance from the center of the cusp (cm)
△ E_0 = 100
● E_0 = 20
rf electrode

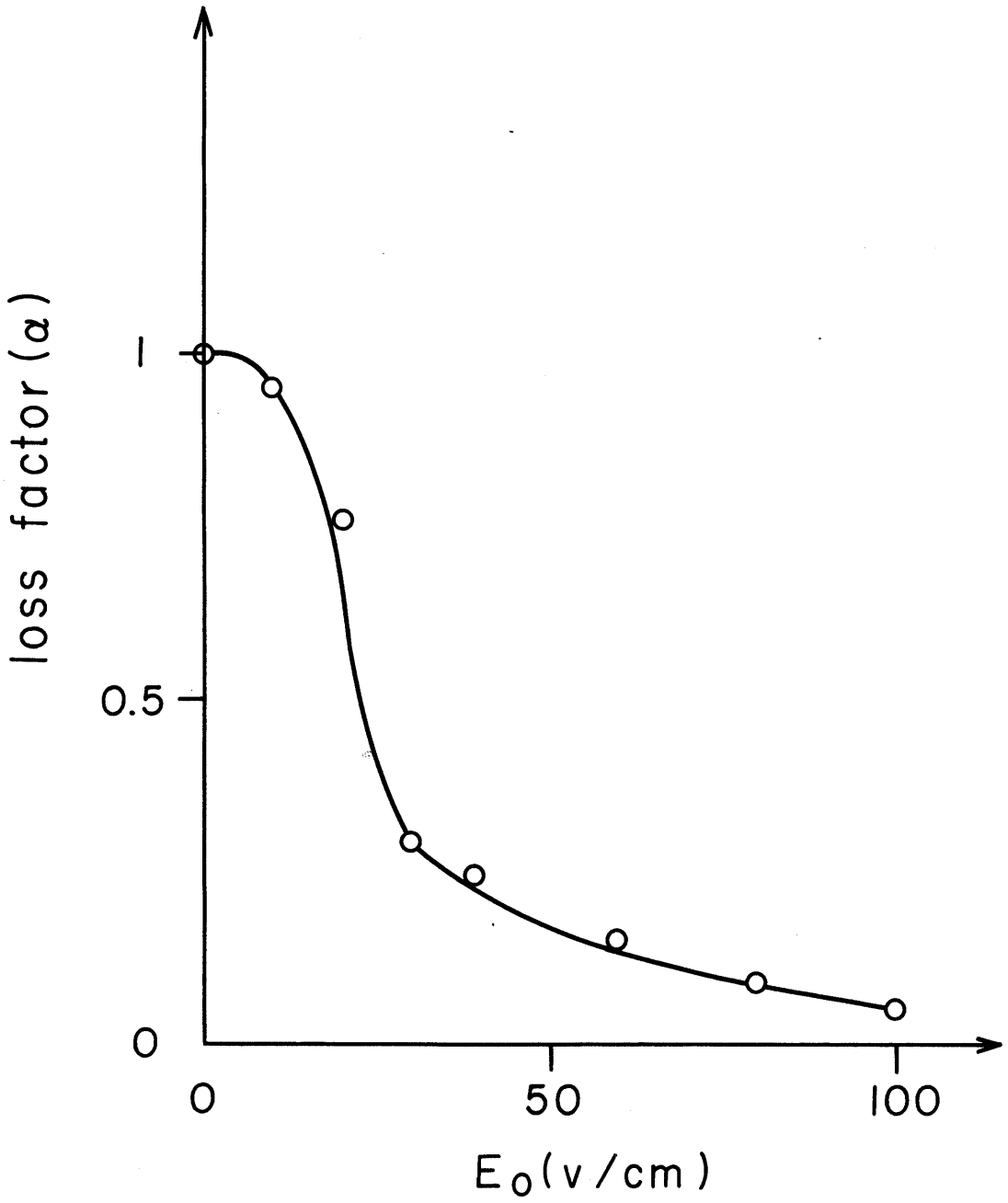
loss factor (α)
1
0.5
0
0
50
100
E_0 (v/cm)

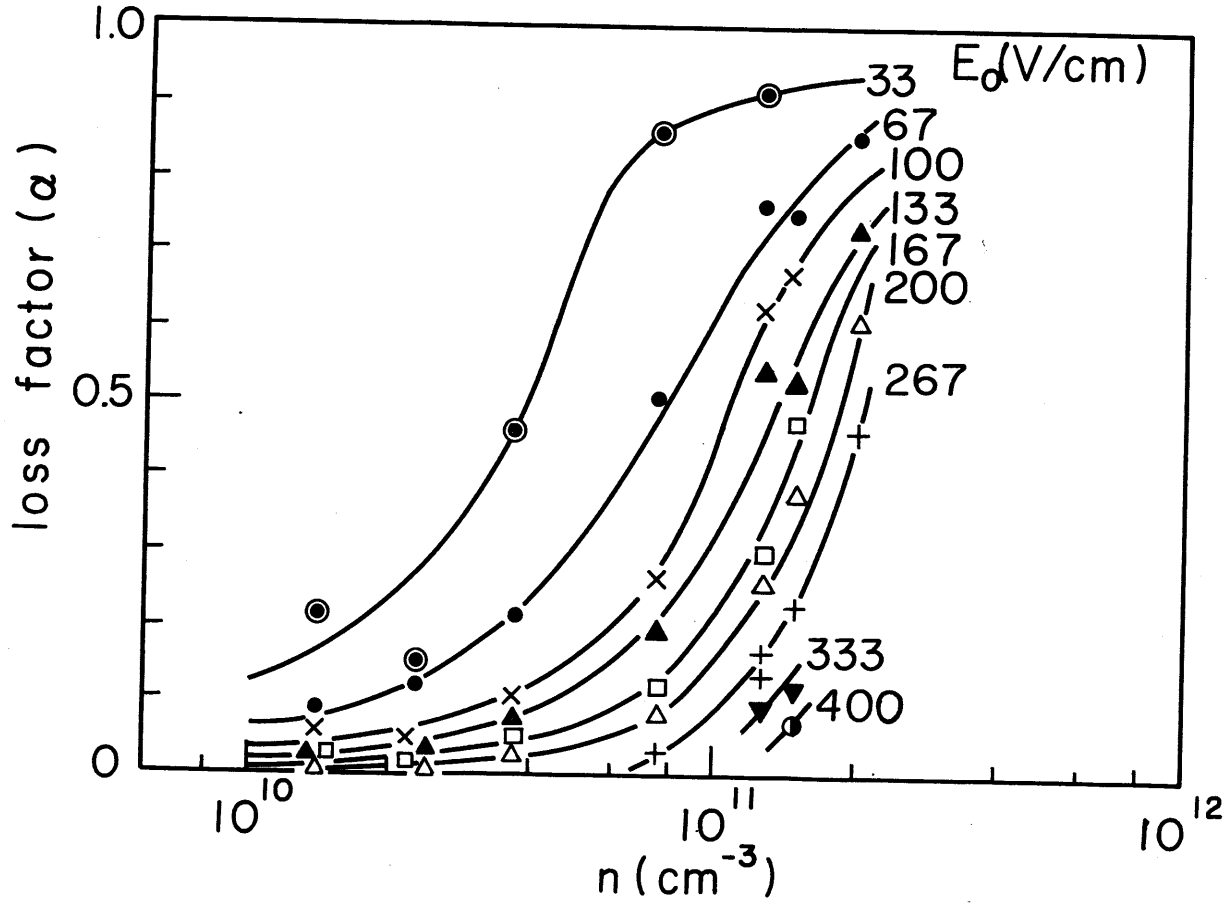
1.0
0.5
0
loss factor (α)
E_0(V/cm)
33
67
100
133
167
200
267
333
400
10^{10}
10^{11}
10^{12}
n (cm^{-3})

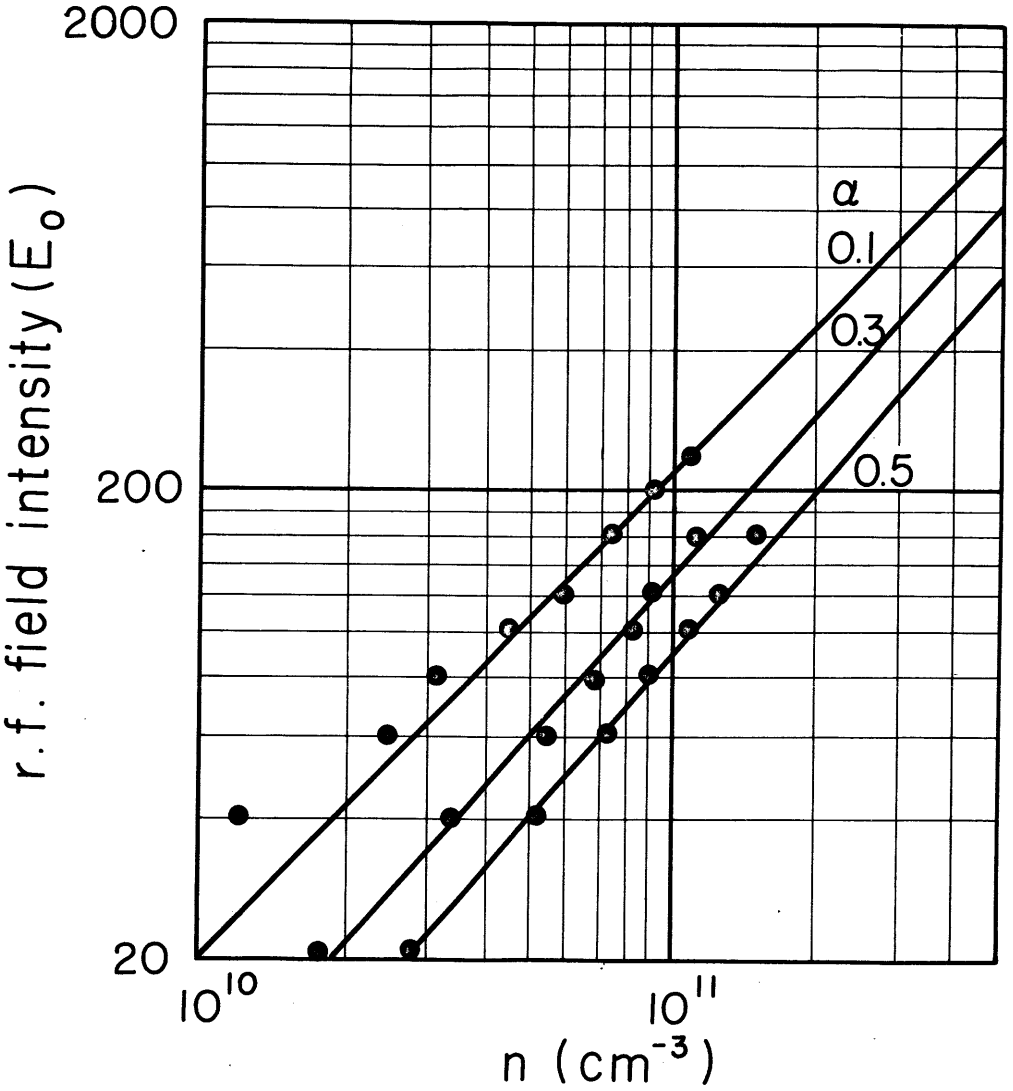
2000
200
20
r.f. field intensity (E_o)
10^{10}
10^{11}
n (cm^{-3})
α
0.1
0.3
0.5